Electrical Power and Energy Systems 80 (2016) 10–25

Contents lists available at ScienceDirect

Electrical Power and Energy Systems

journal homepage: www.elsevier.com/locate/ijepes

Unified power flow controller based reactive power dispatch using oppositional krill herd algorithm

Susanta Dutta [a,*], Pranabesh Mukhopadhyay [a], Provas Kumar Roy [b,*], Debashis Nandi [c]

[a] Department of Electrical Engineering, Dr. B C Roy Engineering College, Durgapur, West Bengal, India
[b] Department of Electrical Engineering, Jalpaiguri Government Engineering College, Jalpaiguri-735102, West Bengal, India
[c] Department of Information Technology, National Institute of Technology, Durgapur, West Bengal, India

ARTICLE INFO

Article history:
Received 21 June 2014
Received in revised form 12 December 2015
Accepted 2 January 2016
Available online 2 February 2016

Keywords:
Optimal reactive power dispatch
Oppositional krill herd algorithm
Differential evolution
Biogeography-based optimization
Unified power flow controller
Flexible AC transmission system

ABSTRACT

In power system, minimizing the power loss in the transmission lines and/or minimizing the voltage deviation at the load buses by controlling the reactive power is referred as optimal reactive power dispatch (ORPD). This paper presents an improved evolutionary algorithm based on oppositional krill herd algorithm (OKHA) for obtaining optimal steady-state performance of power systems. This article also proposes the effect of UPFC location in steady-state analysis and to demonstrate the capabilities of UPFC in controlling active and reactive power flow within any electrical network. To verify the effectiveness of KHA and OKHA, two different single objective functions such as minimization of real power losses and improvement of voltage profile and a multi-objective function that simultaneously minimizes transmission loss and voltage deviation have been studied through standard IEEE 57-bus and 118-bus test systems and their results have been reported. The study results show that the proposed KHA and OKHA approaches are feasible and efficient.

Introduction

Transmission network is the most important component in competitive electricity markets and serves as the key mechanism for generators to compete in the supply to reach large users and distribution companies. In competitive electricity markets [1], energy prices and transmission pricing are highly affected by transmission congestion and other system constraints, where a congested transmission is accompanied by higher costs due to resorting to out-of-merit order as expensive generating units are dispatched to alleviate congestion [2]. Therefore, an increased attention has been paid to new devices that provide more flexibility to operate the transmission system and guarantee lower-cost mechanisms by which transmission constraints can be mitigated.

Available transfer capability (ATC) is the measure of the ability of interconnected electric power systems to reliably move or transfer power from one area to another over all the transmission lines between those areas under specified system conditions [3]. To operate the power system safely and to gain benefits of the bulk power transfer, the transfer capabilities must be calculated and the power system operated so that the power transfers do not exceed the transfer capability. ATC is significantly limited by heavily loaded circuits or buses with relatively low voltages. Flexible AC transmission system (FACTS) technology makes it possible to redistribute line flow and regulate bus voltages. It can be used effectively for the enhancement of ATC.

Continuous and fast improvement of power electronics technology has made FACTS as a promising concept for power system applications during the last decade [4,5]. The use of FACTS controllers provides a flexible controlling of power flow along the transmission lines. It can reduce the flows of heavily loaded lines, maintain the bus voltages at desired levels, and improve the stability of the power network. The UPFC [6,7] is the most versatile FACTS controller envisaged so far. It can not only perform the functions of the STATCOM, TCSC and the phase angle regulator but also provides additional flexibility by combining some of the functions of the above controllers. The UPFC can provide simultaneous control of all basic power system parameters. It can fulfill functions of reactive shunt compensation, series compensation and phase shifting meeting multiple control objectives. From a functional perspective, the objectives are met by applying a boosting transformer injected voltage and an exciting transformer reactive current. The injected voltage is inserted by a series transformer.

In the last decade, various algorithms have been developed for the optimal power flow (OPF) incorporating with UPFC device as well as for the optimal placement of UPFC. Some of them are: a sensitivity based approach which has been developed for finding

* Corresponding authors at: Department of Electrical Engineering, Jalpaiguri Government Engineering College, Jalpaiguri-735102, West Bengal, India. Tel.: +91 9474521395; fax: +91 3561 256143 (P.K. Roy).

E-mail address: roy_provas@yahoo.com (P.K. Roy).

http://dx.doi.org/10.1016/j.ijepes.2016.01.032
0142-0615/

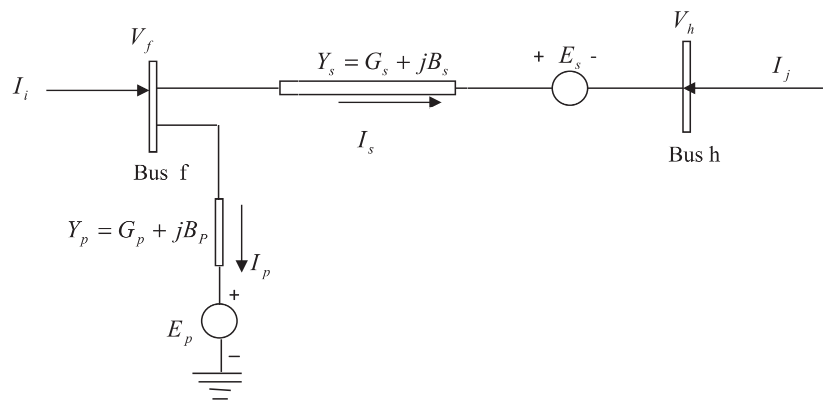

Fig. 1. Circuit model for UPFC.

Table 1
Input parameters setting of different algorithms.

BBO	DE	KHA and OKHA
Mutation probability = 0.005; maximum immigration rate = 1; maximum emigration rate = 1; elitism parameter = 4;	Scaling factor = 0.7 crossover probability = 0.2	Maximum induced speed = 0.01; maximum diffusion speed = 0.05; position factor = 0.2; inertia weight = 0.9; jumping probability = 0.3

suitable placement of UPFC [8], an evolutionary-programming-based load flow algorithm for systems containing UPFC [9], a genetic algorithm (GA) which proposed for solving the optimal location problem of UPFC [10], particle swarm optimization (PSO) for optimal location of FACTS devices [11], etc.

Ara et al. [12] proposed a solution procedure using nonlinear programming (NLP) and mixed-integer nonlinear programming (MINLP) for solving the optimal location and setting of FACTS incorporated in the optimal power-flow problem with the objective functions being considered are the total fuel cost, power losses, and system loadability with and without FACTS installation and improving the power system operation. Sawhney and Jeyasurya [13] presented the application of UPFC to improve the transfer capability of a power system to meet some of the challenges of power system operation caused by deregulation in the electric power industry and opening of the market for delivery of cheaper energy to the customers. Alomoush [14] developed a mathematical approach allocating the contributions of UPFCs to transmission system usage by making use of a dc-based load flow model of UPFC-inserted transmission lines based on a previously derived dc-based injection model of UPFC-embedded lines. Relationships were derived to model the impact of UPFC on line flows and transmission usage by using modified admittances and distribution factors that model impact of utilizing UPFC on line flows and system usage. Taher and Amooshahi [15] presented the application of hybrid immune algorithm (HIA) such as immune GA (IGA) and immune PSO (IPSO) to find optimal location of UPFC to achieve optimal performance of power system. Simulations were performed on IEEE 14-bus and IEEE 30-bus test systems considering the overall cost function as the objective function, including the total active and reactive production cost function of the generators and installation cost of UPFCs. Shaheen et al. [16] presented a new

Table 2
Simulation result of different algorithms for loss minimization (IEEE 57-bus system without UPFC).

Control variables	BBO	DE	KHA	OKHA	Control variables	BBO	DE	KHA	OKHA
V_{g1} (p.u.)	1.0599	1.0598	1.0597	1.0600	T_{24-26}	1.0322	1.0285	1.0328	1.0272
V_{g2} (p.u.)	1.0514	1.0483	1.0526	1.0581	T_{7-29}	0.9233	0.9141	0.9285	0.9497
V_{g3} (p.u.)	1.0186	1.0103	1.0241	1.0415	T_{34-32}	0.9203	0.9177	0.9351	0.9303
V_{g6} (p.u.)	0.9964	0.9861	1.0020	1.0249	T_{11-41}	0.9004	0.9107	0.9041	0.9033
V_{g8} (p.u.)	1.0175	1.0083	1.0230	1.0442	T_{15-45}	0.9359	0.9292	0.9440	0.9580
V_{g9} (p.u.)	0.9944	0.9785	1.0013	1.0223	T_{14-46}	0.9203	0.9040	0.9159	0.9349
V_{g12} (p.u.)	1.0061	1.0000	1.0129	1.0386	T_{10-51}	0.9295	0.9164	0.9297	0.9526
Q_{C18} (p.u.)	0.0875	0.0139	0.0972	0.0710	T_{13-49}	0.9010	0.9017	0.9001	0.9209
Q_{C25} (p.u.)	0.0589	0.0589	0.0590	0.0589	T_{11-43}	0.9159	0.9112	0.9157	0.9405
Q_{C53} (p.u.)	0.0629	0.0617	0.0627	0.0630	T_{40-56}	1.0220	1.0497	1.0314	1.0250
T_{4-18}	0.9604	0.9185	0.9905	1.0157	T_{39-57}	0.9624	0.9879	0.9862	0.9792
T_{4-18}	0.9193	0.9197	0.9102	0.9120	T_{9-55}	0.9282	0.9126	0.9358	0.9540
T_{21-20}	1.0033	1.0102	1.0174	1.0153					

	BBO	DE	KHA	OKHA
Loss (MW)	40.5535	41.3003	40.2431	39.8134
Voltage deviation (p.u.)	1.2973	1.3643	1.3150	1.3736
Computational time (s)	16.6843	13.6934	4.8806	4.5349

Table 3
Simulation result of different algorithms for loss minimization (IEEE 57-bus system with UPFC).

Control variables	BBO	DE	KHA	OKHA	Control variables	BBO	DE	KHA	OKHA
V_{g1} (p.u.)	1.0597	1.0575	1.0597	1.0598	T_{24-26}	1.0268	1.0366	1.0357	1.0360
V_{g2} (p.u.)	1.0543	1.0433	1.0578	1.0550	T_{7-29}	0.9315	0.9243	0.9366	0.9403
V_{g3} (p.u.)	1.0260	1.0156	1.0374	1.0312	T_{34-32}	0.9254	0.9227	0.9398	0.9350
V_{g6} (p.u.)	1.0067	0.9986	1.0132	1.0146	T_{11-41}	0.9711	0.9065	0.9006	0.9002
V_{g8} (p.u.)	1.0244	1.0191	1.0318	1.0360	T_{15-45}	0.9434	0.9331	0.9576	0.9488
V_{g9} (p.u.)	0.9981	0.9915	1.0196	1.0098	T_{14-46}	0.9164	0.9113	0.9310	0.9211
V_{g12} (p.u.)	1.0105	1.0042	1.0396	1.0215	T_{10-51}	0.9251	0.9233	0.9523	0.9397
Q_{C18} (p.u.)	0.0964	0.0986	0.0997	0.0976	T_{13-49}	0.9004	0.9028	0.9057	0.9154
Q_{C25} (p.u.)	0.0587	0.0586	0.0590	0.0589	T_{11-43}	0.9071	0.9151	0.9381	0.9251
Q_{C53} (p.u.)	0.0626	0.0626	0.0622	0.0629	T_{40-46}	1.0560	1.0102	1.0110	1.0304
T_{4-18}	0.9762	0.9671	1.0142	0.9079	T_{39-57}	0.9828	0.9763	0.9685	0.9824
T_{4-18}	0.9239	0.9289	0.9165	0.9895	T_{9-55}	0.9339	0.9258	0.9618	0.9424
T_{21-20}	1.0139	1.0171	1.0218	1.0144					

	BBO	DE	KHA	OKHA
Active power injected by UPFC (p.u.)				
Sending end	0.0138	0.0224	0.0316	0.0123
Receiving end	0.0286	0.0236	0.0197	0.0147
Reactive power injected by UPFC (p.u.)				
Sending end	0.0315	−0.0193	0.0317	0.0139
Receiving end	−0.0247	−0.0054	0.0278	0.0340
Optimal location and parameters of UPFC				
Optimal position	22–38	35–36	35–36	25–30
Series source voltage (p.u.)	0.0436	0.0393	0.0567	0.0581
Series source phase angle (rad)	−0.1346	−0.2847	−0.1336	−0.2450
Shunt source voltage (p.u.)	1.0346	1.0127	1.0562	1.0493
Shunt source phase angle (rad)	−0.2858	−0.3642	−0.4875	0.3008
Loss (MW)	39.3640	40.7651	39.3642	38.4255
Voltage deviation (p.u.)	1.3549	1.3143	1.3489	1.4056
Computational time (s)	17.5782	14.9003	4.9655	4.7538

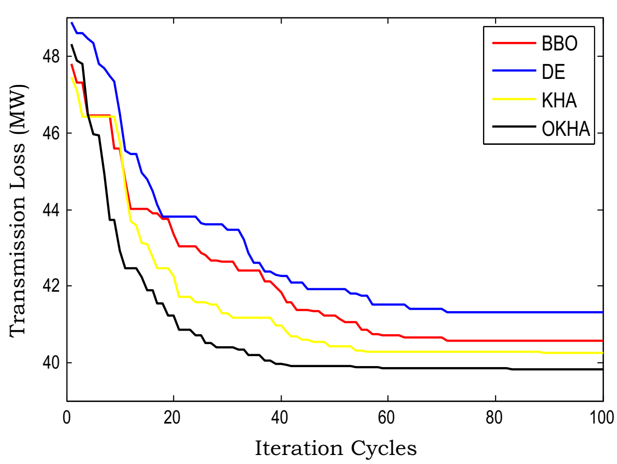

Fig. 2. Transmission loss convergence graph using different algorithms of IEEE 57-bus without UPFC.

approach based on differential evolution (DE) technique to find out the optimal placement and parameter setting of UPFC for enhancing power system security under single line contingencies. Vural and Tümay [17] focused on the mathematical modeling of UPFC for the implementation of the device in conventional Newton–Raphson (NR) power flow algorithm and in power system analysis software package (PSASP). Visakha et al. [18] presented an approach for selecting suitable locations of UPFC considering normal and network contingencies after evaluating the degree of severity of the contingencies.. Roy et al. proposed biogeography based optimization (BBO) [19] to solve TCSC and TCPS based optimal reactive power dispatch (ORPD) problem for minimizing voltage deviation and transmission loss of IEEE 30-bus test system. Panda [20] investigated the application of non-dominated sorting in genetic algorithms-II (NSGA-II) technique for designing a FACTS based controller to improve the stability of the power system with minimum control effort. The proposed technique was applied for generating a Pareto set of global optimal solutions to the multi-objective optimization problem. Furthermore, the best compromise solution from the obtained Pareto solution set was chosen by using a fuzzy-based membership value assignment method. Edward et al. [21] developed an enhanced bacterial foraging algorithm (EBFA) by including Nelder–Mead (NM) algorithm to conventional bacterial foraging algorithm (BFA) for better performance of power system. This was done to overcome the difficulty of optimal parameter selection of the conventional BFA technique. Hassan et al. proposed GA [22] technique for the stabilization of power systems using UPFC devices. Kumar et al. presented cat swarm optimization (CSO) approach [23] for the optimal location and sizing of UPFC in transmission system to improve the voltage profile and maximum loading parameter.

From the literature it is observed that UPFC device has hardly been used to solve optimal reactive power dispatch (ORPD) problem. This motivates the authors to incorporate UPFC to solve ORPD problems. In this study, two different objectives of ORPD namely minimization of transmission loss and minimization of voltage deviations are considered. In recent years, a new optimization technique named krill herd algorithm (KHA) inspired by herding behavior of krill individual firstly presented by Gandomi in 2012, has been successfully applied in various field of engineering. In this article, KHA algorithm is employed to find optimal location of UPFC for solving ORPD problem. Moreover, to improve the solution quality and convergence speed, opposition based learning is integrated with the conventional KHA algorithm. In order to show the effectiveness of the proposed KHA and OKHA approaches, two Standard test systems of IEEE 57-bus and IEEE 118-bus are used in this

Table 4
Simulation result of different algorithms for voltage deviation minimization (IEEE 57-bus system without UPFC).

Control variables	BBO	DE	KHA	OKHA	Control variables	BBO	DE	KHA	OKHA
V_{g1} (p.u.)	1.0134	1.0385	1.0209	1.0157	T_{24-26}	1.0897	1.0761	1.0863	1.0898
V_{g2} (p.u.)	0.9580	0.9686	0.9563	0.9929	T_{7-29}	0.9325	0.9245	0.9355	0.9306
V_{g3} (p.u.)	1.0294	1.0189	1.0382	1.0248	T_{34-32}	0.9004	0.9007	0.9005	0.9001
V_{g6} (p.u.)	1.0003	0.9935	0.9970	0.9863	T_{11-41}	0.9118	0.9113	0.9000	0.9003
V_{g8} (p.u.)	1.0373	1.0436	1.0416	1.0468	T_{15-45}	0.9282	0.9185	0.9396	0.9267
V_{g9} (p.u.)	0.9800	0.9828	0.9921	1.0001	T_{14-46}	0.9248	0.9162	0.9101	0.9361
V_{g12} (p.u.)	1.0309	1.0029	1.0156	1.0258	T_{10-51}	0.9862	0.9752	0.9799	0.9760
Q_{C18} (p.u.)	0.0310	0.0559	0.0551	0.0157	T_{13-49}	0.9026	0.9170	0.9025	0.9022
Q_{C25} (p.u.)	0.0587	0.0586	0.0587	0.0580	T_{11-43}	0.9135	0.9105	0.9185	0.9183
Q_{C53} (p.u.)	0.0629	0.0627	0.0619	0.0627	T_{40-56}	1.0580	1.0939	0.9901	1.0103
T_{4-18}	0.9915	0.9747	1.0406	0.9690	T_{39-57}	0.9065	0.9591	0.9013	0.9020
T_{4-18}	0.9388	0.9455	0.9237	0.9362	T_{9-55}	0.9504	0.9755	0.9013	0.9735
T_{21-20}	0.9924	0.9904	0.9963	0.9907					

	BBO	DE	KHA	OKHA
Loss (MW)	52.6068	50.4412	52.8884	46.4442
Voltage deviation (p.u.)	1.0409	1.1104	1.0182	0.9954
Computational time (s)	16.4293	13.6540	4.1813	4.0359

Table 5
Simulation result of different algorithms for voltage deviation minimization (IEEE 57-bus system with UPFC).

Control variables	BBO	DE	KHA	OKHA	Control variables	BBO	DE	KHA	OKHA
V_{g1} (p.u.)	1.0179	1.0129	1.0178	1.0147	T_{24-26}	1.0901	1.0877	1.0877	1.0899
V_{g2} (p.u.)	0.9465	0.9643	0.9860	1.0165	T_{7-29}	0.9172	0.9334	0.9327	0.9322
V_{g3} (p.u.)	1.0289	1.0158	1.0232	1.0328	T_{34-32}	0.9005	0.9015	0.9005	0.9003
V_{g6} (p.u.)	1.0007	1.0028	1.0018	0.9954	T_{11-41}	0.9005	0.9082	0.9046	0.9003
V_{g8} (p.u.)	1.0123	1.0360	1.0354	1.0407	T_{15-45}	0.9380	0.9216	0.9297	0.9304
V_{g9} (p.u.)	1.0017	0.9926	0.9984	1.0031	T_{14-46}	0.9206	0.9332	0.9202	0.9179
V_{g12} (p.u.)	1.0240	1.0310	1.0236	1.0260	T_{10-51}	0.9813	0.9662	0.9888	0.9714
Q_{C18} (p.u.)	0.0135	0.0526	0.0226	0.0949	T_{13-49}	0.9093	0.9038	0.9008	0.9273
Q_{C25} (p.u.)	0.0588	0.0587	0.0590	0.0588	T_{11-43}	0.9191	0.9151	0.9178	0.9234
Q_{C53} (p.u.)	0.0629	0.0613	0.0625	0.0623	T_{40-46}	0.9992	1.0442	0.9944	0.9879
T_{4-18}	0.9573	1.0243	0.9119	0.9165	T_{39-57}	0.9004	0.9088	0.9002	0.9032
T_{4-18}	0.9551	0.9125	0.9920	1.0316	T_{9-55}	0.9753	0.9607	0.9673	0.9734
T_{21-20}	0.9937	0.9922	0.9922	0.9941					

	BBO	DE	KHA	OKHA
Active power injected by UPFC (p.u.)				
Sending end	0.0247	0.0185	0.0118	0.0480
Receiving end	0.0313	0.0192	0.0347	0.0247
Reactive power injected by UPFC (p.u.)				
Sending end	0.0462	0.0098	−0.0291	0.0377
Receiving end	−0.0271	0.0143	−0.0185	−0.0124
Optimal location and parameters of UPFC				
Optimal position	27–28	7–29	11–41	11–41
Series source voltage(rad)	0.0471	0.0356	0.0612	0.0388
Series source phase angle (rad)	−0.1237	−0.2134	−0.2703	−0.1426
Shunt source voltage (p.u.)	1.0342	1.0212	1.0178	1.0642
Shunt source phase angle(rad)	−0.1741	−0.3148	−0.1346	−0.2641
Loss (MW)	55.0266	48.3641	47.3965	46.3822
Voltage deviation (p.u.)	0.9743	1.0249	0.9278	0.8942
Computational time (s)	17.1538	14.5427	4.3796	4.1847

paper. Results obtained from the proposed approaches are compared with those obtained from biogeography based optimization (BBO) and DE.

The rest of the paper is organized as follows. In section 'Problem formulation', the problem formulation is presented. In section 'Algorithms', KHA, OKHA algorithms along with BBO, DE algorithms are briefly explained. In section 'Oppositional krill herd algorithm applied to ORPD problem', OKHA developed for ORPD problems is described. In section 'Simulation results and discussion', the studies of application cases are presented and demonstrate the potential of the proposed KHA and OKHA algorithms. Finally, in section 'Conclusion', the conclusions are given.

Problem formulation

Modeling of UPFC in power system under steady state operation

The most versatile FACTS device presently available for transmission system control is capable of providing active and reactive load flow control between its terminals. It may also provide reactive power compensation to the node to which it is connected [3,4]. UPFC can be divided into two FACTS controllers; first one is series controller and second one shunt controller. Series controller is equivalent to the SSSC and shunt controller is equivalent to STATCOM. When the STATCOM and the SSSC operate as standalone

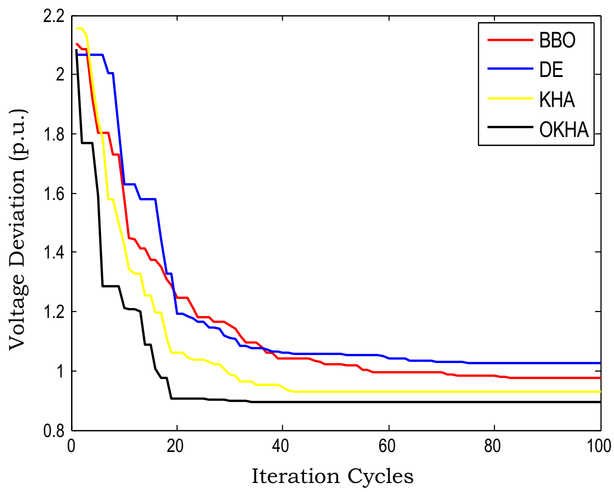

Fig. 3. Voltage deviation convergence graph using different algorithms of IEEE 57-bus with UPFC.

FACTS controllers, they exchange almost exclusively reactive power at their terminals. During the stand-alone operations, the SSSC injects a voltage in quadrature with the line current, thereby emulating an inductive and capacitive reactance at the point of compensation in series with the line, and the STATCOM injects a reactive current, thereby also emulating a reactance at the point of compensation in shunt with the line. In the steady state operation, the main objective of an UPFC is to simultaneously control the active and reactive power flow through the transmission line and bus voltage at which shunt component of the UPFC is connected. The basic schematic and power injection model of the UPFC are presented in Fig. 1. Using the power injection model of UPFC, the following formulation can be extracted

$$P_f = P_{fh} + \sum_{j=1}^{N} |V_f||V_j||Y_{fj}| \cos(\delta_f - \delta_j - \theta_{fj}) \tag{1}$$

$$Q_f = Q_{fh} + \sum_{j=1}^{N} |V_f||V_j||Y_{fj}| \sin(\delta_f - \delta_j - \theta_{fj}) \tag{2}$$

$$P_h = P_{hf} + \sum_{j=1}^{N} |V_h||V_j||Y_{hj}| \cos(\delta_h - \delta_j - \theta_{hj}) \tag{3}$$

$$Q_h = Q_{hf} + \sum_{j=1}^{N} |V_h||V_j||Y_{hj}| \sin(\delta_h - \delta_j - \theta_{hj}) \tag{4}$$

The active and the reactive power flow through the transmission line connected between the fth and the hth bus having UPFC may be derived as follows [24]:

$$\begin{aligned} P_{fh} = {} & |V_f|^2 (G_p + G_s) - |V_f||E_p||Y_p| \cos(\theta_p - \delta_f + \delta_p) \\ & - |V_f||V_h||Y_s| \cos(\theta_s - \delta_f + \delta_h) \\ & + |V_f||E_s||Y_s| \cos(\theta_s - \delta_f + \delta_s) \end{aligned} \tag{5}$$

$$\begin{aligned} Q_{fh} = {} & -|V_f|^2 (B_p + B_s) + |V_f||E_p||Y_p| \sin(\theta_p - \delta_f + \delta_p) \\ & + |V_f||V_h||Y_s| \sin(\theta_s - \delta_f + \delta_h) \\ & - |V_f||E_s||Y_s| \sin(\theta_s - \delta_f + \delta_s) \end{aligned} \tag{6}$$

$$\begin{aligned} P_{hf} = {} & |V_h|^2 G_s - |V_h||E_s||Y_s| \cos(\theta_s - \delta_h + \delta_s) \\ & - |V_h||V_f||Y_s| \cos(\theta_s - \delta_h + \delta_f) \end{aligned} \tag{7}$$

$$\begin{aligned} Q_{hf} = {} & -|V_h|^2 B_s + |V_h||E_s||Y_s| \sin(\theta_s - \delta_h + \delta_s) \\ & + |V_h||V_f||Y_s| \sin(\theta_s - \delta_h + \delta_f) \end{aligned} \tag{8}$$

where V_f, V_h are the voltage magnitudes at the fth and the hth bus, respectively; Y_p is the admittance of the parallel component; G_p, B_p are the conductance and susceptance, respectively, of the parallel components; Y_s is the summation of the admittance of the transmission line connected between the fth bus and the admittance of the series component of the UPFC; G_s, B_s are the conductance and susceptance, respectively, of the series components of UPFC; θ_s is the admittance angle of the admittance that includes the admittance of the line k-m and the admittance of the series component of the UPFC; δ_p, δ_s are the voltage source angle of the parallel and series components of the UPFC; E_p, E_s are the voltage sources of parallel and series converters, respectively, of the UPFC devices.

Objective functions

The main objective of ORPD problem goal is to minimize active power losses and improve the voltage profile by setting generator bus voltages, VAR compensators, and transformer taps. Therefore, the objectives of ORPD may be expressed as follows:

Table 6
Simulation result of different algorithms for simultaneous minimization of loss and voltage deviation (IEEE 57-bus system without UPFC).

Control variables	BBO	DE	KHA	OKHA	Control variables	BBO	DE	KHA	OKHA
V_{g1} (p.u.)	1.0599	1.0596	1.0513	1.0550	T_{24-26}	0.9995	0.9826	1.0911	1.0815
V_{g2} (p.u.)	1.0383	1.0397	1.0251	1.0490	T_{7-29}	0.9301	0.9294	0.9300	0.9263
V_{g3} (p.u.)	1.0142	1.0213	1.0165	1.0153	T_{34-32}	0.9040	0.9068	0.9030	0.9005
V_{g6} (p.u.)	0.9976	1.0114	0.9912	0.9988	T_{11-41}	0.9101	0.9098	0.9056	0.9094
V_{g8} (p.u.)	0.9998	1.0151	1.0432	1.0304	T_{15-45}	0.9002	0.9008	0.9187	0.9231
V_{g9} (p.u.)	0.9804	0.9954	1.0267	1.0312	T_{14-46}	0.9000	0.9012	0.9366	0.9063
V_{g12} (p.u.)	1.0266	1.0368	1.0163	1.0019	T_{10-51}	0.9838	1.0010	1.0030	1.0000
Q_{C18} (p.u.)	0.0999	0.0995	0.0036	0.0892	T_{13-49}	0.9121	0.9386	0.9141	0.9151
Q_{C25} (p.u.)	0.0589	0.0589	0.0558	0.0578	T_{11-43}	0.9247	0.9380	0.9211	0.9375
Q_{C53} (p.u.)	0.0629	0.0623	0.0587	0.0623	T_{40-56}	0.9171	0.9283	0.9947	1.0860
T_{4-18}	0.9372	0.9551	0.9487	0.9731	T_{39-57}	0.9081	0.9097	1.0058	0.9552
T_{4-18}	0.9392	0.9395	0.9601	1.0198	T_{9-55}	0.9345	0.9637	0.9998	0.9923
T_{21-20}	1.0107	1.0103	0.9719	0.9588					

	BBO	DE	KHA	OKHA
Loss (MW)	42.6822	42.3936	42.3319	42.0575
Voltage deviation (p.u.)	1.2558	1.2680	1.0196	1.0101
Computational time (s)	16.5361	13.5213	4.1602	4.0623

Table 7
Simulation result of different algorithms for simultaneous minimization of loss and voltage deviation (IEEE 57-bus system with UPFC).

Control variables	BBO	DE	KHA	OKHA	Control variables	BBO	DE	KHA	OKHA
V_{g1} (p.u.)	1.0537	1.0440	1.0537	1.0467	T_{24-26}	1.0836	1.0982	1.0817	1.0937
V_{g2} (p.u.)	1.0512	1.0316	1.0449	1.0441	T_{7-29}	0.9361	0.9281	0.9361	0.9248
V_{g3} (p.u.)	1.0199	1.0210	1.0211	1.0196	T_{34-32}	0.9007	0.9006	0.9002	0.9016
V_{g6} (p.u.)	0.9978	0.9983	1.0022	1.0152	T_{11-41}	0.9062	0.9014	0.9062	0.9172
V_{g8} (p.u.)	1.0408	1.0358	1.0336	1.0288	T_{15-45}	0.9108	0.9025	0.9108	0.9273
V_{g9} (p.u.)	1.0299	1.0359	1.0335	1.0296	T_{14-46}	0.9473	0.9498	0.9543	0.9271
V_{g12} (p.u.)	1.0003	1.0023	1.0003	1.0080	T_{10-51}	0.9832	1.0018	0.9828	0.9904
Q_{C18} (p.u.)	0.0246	0.0618	0.0236	0.0631	T_{13-49}	0.9017	0.9079	0.9017	0.9012
Q_{C25} (p.u.)	0.0581	0.0585	0.0583	0.0566	T_{11-43}	0.9066	0.9195	0.9042	0.9267
Q_{C53} (p.u.)	0.0602	0.0581	0.0619	0.0465	T_{40-46}	1.0617	1.0379	1.0605	1.0161
T_{4-18}	1.0036	0.9462	1.0199	0.9181	T_{39-57}	0.9036	0.9222	0.9188	0.9593
T_{4-18}	0.9436	1.0174	0.9591	1.0687	T_{9-55}	0.9968	1.0100	0.9946	1.0223
T_{21-20}	0.9866	0.9781	0.9731	0.9879					

	BBO	DE	KHA	OKHA
Active power injected by UPFC (p.u.)				
Sending end	0.0340	0.0718	0.0483	0.0664
Receiving end	0.0387	0.0699	0.0518	0.0684
Reactive power injected by UPFC (p.u.)				
Sending end	0.0317	−0.0813	0.0347	−0.0196
Receiving end	0.0293	0.0545	−0.0303	0.0082
Optimal location and parameters of UPFC				
Optimal position	12–17	19–20	12–17	12–16
Series source voltage (rad)	0.0359	0.0611	0.0238	0.0529
Series source phase angle (rad)	−0.0128	−0.0106	−0.0333	−0.1320
Shunt source voltage (p.u.)	1.0362	1.0271	1.0316	1.0118
Shunt source phase angle (rad)	−0.0916	−0.0754	−0.0551	−0.0782
Loss (MW)	41.3703	41.7006	41.0127	40.7324
Voltage deviation (p.u.)	1.2117	1.2067	0.9875	0.0328
Computational time (s)	18.0723	14.8143	4.6327	4.1710

Active power loss minimization

The primary objective of ORPD is minimization of network active power loss, while satisfying the operating constraints. This objective function may be expressed as:

$$f_1 = \min(P_{loss}) = \min\left[\sum_{k=1}^{N_{TL}} G_p\left(V_f^2 + V_h^2 - 2V_f V_h \cos\theta_{fh}\right)\right] \quad (9)$$

where P_{loss} is the total active power loss; G_P is the conductance of the pth branch connected between them fth and hth bus; θ_{fh} is the admittance angle of the transmission line connected between them fth and hth bus; N_{TL} is the number of transmission lines; V_f, V_h are the voltage magnitudes of fth and hth bus, respectively.

Voltage profile improvement

Minimization of deviations of voltages from desired values is required since bus voltage is one of the most important security and service quality indexes. The objective function of voltage profile improvement, i.e. voltage deviation minimization at load buses, maybe expressed as:

$$f_2 = \min\left(\sum_{f=1}^{N_L}\left|V_{L_f} - V_{L_f}^{sp}\right|\right) \quad (10)$$

where V_{L_f} is the voltage at the fth load bus; $V_{L_f}^{SP}$ is the desired voltage at the fth load bus, usually set to 1.0 p.u.

Simultaneous minimization of transmission loss and voltage deviation

In order to judge the effectiveness, the proposed method is also applied to solve multi-objective ORPD problem. In multi-objective optimization problem, a multiple objectives are optimized simultaneously while satisfying various equality and inequality constraints. In this article, to implement multi-objective OKH algorithm for minimizing both transmission loss and voltage deviation simultaneously, price penalty factor approach is introduced to find the best compromising solutions. To improve the voltage profile and to reduce the transmission loss, the objective function may be described as follows:

$$f_3 = f_1 + pf \times f_2 \quad (11)$$

where f_3 is the combined voltage deviation and transmission loss minimization objective function; f_1, f_2 are the transmission loss and voltage deviation minimization objective, and pf is the price penalty factor.

System constraints

Equality constraint

The equality constraints of the ORPD problem are the active and reactive power balance equations. These are given by:

$$P_{G_f} - P_{D_f} - V_f\sum_{h=1}^{N_B} V_h\left[G_{fh}\cos\left(\theta_f - \theta_h\right) + B_{fh}\sin\left(\theta_f - \theta_h\right)\right] = 0,$$
$$f = 1, \ldots, N_B \quad (12)$$

$$Q_{G_f} - Q_{D_f} - V_f\sum_{h=1}^{N_B} V_h\left[G_{fh}\sin\left(\theta_f - \theta_h\right) - B_{fh}\cos\left(\theta_f - \theta_h\right)\right] = 0,$$
$$f = 1, \ldots, N_B \quad (13)$$

where G_{fh}, B_{fh} are the real and imaginary part of the bus admittance matrix of the transmission line connected between them fth and hth bus; P_{G_f}, Q_{G_f} are the active and reactive power generation of the fth bus; P_{D_f}, Q_{D_f} are the active and reactive load demands of the fth bus.

Table 8
Simulation result of different algorithms for loss minimization (IEEE 118-bus system without UPFC).

Control variables	BBO	DE	KHA	OKHA	Control variables	BBO	DE	KHA	OKHA
V_{g1} (p.u.)	1.0860	1.0593	1.0898	1.0867	V_{g89} (p.u.)	1.0588	1.0946	1.0484	1.0889
V_{g4} (p.u.)	1.0267	1.0458	1.0169	1.0300	V_{g90} (p.u.)	1.0135	1.0737	1.0070	1.0626
V_{g6} (p.u.)	1.0486	1.0484	1.0444	1.0571	V_{g91} (p.u.)	1.0064	1.0684	0.9983	1.0630
V_{g8} (p.u.)	1.0409	1.0481	1.0333	1.0485	V_{g92} (p.u.)	1.0231	1.0635	1.0136	1.0683
V_{g10} (p.u.)	1.0116	1.0340	1.0467	1.0524	V_{g99} (p.u.)	1.0187	1.0265	1.0449	1.0431
V_{g12} (p.u.)	1.0818	1.0797	1.0676	1.0678	V_{g100} (p.u.)	1.0259	1.0214	1.0533	1.0470
V_{g15} (p.u.)	1.0384	1.0522	1.0270	1.0403	V_{g103} (p.u.)	1.0301	0.9941	1.0416	1.0278
V_{g18} (p.u.)	1.0190	1.0301	1.0096	1.0272	V_{g104} (p.u.)	1.0394	0.9798	1.0340	1.0114
V_{g19} (p.u.)	1.0101	1.0250	1.0169	1.0360	V_{g105} (p.u.)	1.0429	0.9898	1.0263	1.0064
V_{g24} (p.u.)	1.0141	1.0242	1.0128	1.0311	V_{g107} (p.u.)	1.0701	0.9788	1.0125	0.9943
V_{g25} (p.u.)	1.0392	1.0372	1.0553	1.0446	V_{g110} (p.u.)	1.0214	0.9956	1.0243	1.0014
V_{g26} (p.u.)	1.0803	1.0983	1.0970	1.0755	V_{g111} (p.u.)	1.0289	1.0004	1.0338	1.0099
V_{g27} (p.u.)	1.0744	1.0438	1.0875	1.0755	V_{g112} (p.u.)	0.9969	0.9747	1.0051	0.9783
V_{g31} (p.u.)	0.9913	1.0189	1.0389	1.0630	V_{g113} (p.u.)	1.0210	1.0387	1.0245	1.0494
V_{g32} (p.u.)	0.9937	1.0228	1.0275	1.0443	V_{g116} (p.u.)	1.0528	0.9955	1.0507	1.0531
V_{g34} (p.u.)	0.9864	1.0097	1.0350	1.0554	QC_5 (p.u.)	−0.0176	−0.1516	−0.2238	−0.2609
V_{g36} (p.u.)	1.0062	1.0029	1.0440	1.0488	QC_{34} (p.u.)	0.0632	0.0472	0.1301	0.0489
V_{g40} (p.u.)	0.9972	1.0115	1.0422	1.0462	QC_{37} (p.u.)	−0.0160	−0.0161	−0.0021	−0.0005
V_{g42} (p.u.)	1.0058	1.0274	1.0322	1.0290	QC_{44} (p.u.)	0.0980	0.0921	0.0970	0.0985
V_{g46} (p.u.)	1.0270	1.0371	1.0400	1.0425	QC_{45} (p.u.)	0.0995	0.0651	0.0994	0.0978
V_{g49} (p.u.)	1.0468	1.0410	1.0780	1.0794	QC_{46} (p.u.)	0.0095	0.0849	0.0770	0.0098
V_{g54} (p.u.)	1.0792	1.0604	1.0803	1.0858	QC_{48} (p.u.)	0.0016	0.0327	0.0048	0.0003
V_{g55} (p.u.)	1.0607	0.9969	1.0253	1.0219	QC_{74} (p.u.)	0.0476	0.0327	0.0274	0.0860
V_{g56} (p.u.)	1.0604	1.0011	1.0239	1.0191	QC_{79} (p.u.)	0.1957	0.0314	0.1935	0.2000
V_{g59} (p.u.)	1.0612	0.9970	1.0230	1.0205	QC_{82} (p.u.)	0.1958	0.11380.	0.1928	0.1940
V_{g61} (p.u.)	1.0814	1.0178	1.0600	1.0578	QC_{83} (p.u.)	0.0989	0.0940	0.0976	0.0992
V_{g62} (p.u.)	1.0565	0.9868	1.0622	1.0558	QC_{105} (p.u.)	0.1853	0.1340	0.0613	0.0024
V_{g65} (p.u.)	1.0507	1.0009	1.0560	1.0529	QC_{107} (p.u.)	0.0472	0.0411	0.0429	0.0262
V_{g66} (p.u.)	1.0604	0.9990	1.0445	1.0640	QC_{110} (p.u.)	0.0107	0.0032	0.0147	0.0528
V_{g69} (p.u.)	1.0880	1.0266	1.0851	1.0962	T_{8-5}	0.9946	0.9921	0.9806	0.9844
V_{g70} (p.u.)	1.0470	1.0061	1.0411	1.0397	T_{26-25}	1.0992	1.0114	1.0987	1.0983
V_{g72} (p.u.)	1.0438	1.0245	1.0408	1.0316	T_{30-17}	1.0105	0.9546	1.0295	0.9877
V_{g73} (p.u.)	1.0488	1.0050	1.0386	1.0371	T_{38-37}	1.0467	0.9082	0.9819	0.9919
V_{g74} (p.u.)	1.0347	0.9721	1.0297	1.0277	T_{63-59}	0.9483	0.9443	0.9661	0.9768
V_{g76} (p.u.)	1.0178	0.9669	1.0261	1.0199	T_{64-61}	1.0020	0.9889	0.9937	0.9982
V_{g77} (p.u.)	1.0217	1.0276	1.0480	1.0423	T_{65-66}	1.0889	1.0483	1.0760	1.0997
V_{g80} (p.u.)	1.0242	1.0410	1.0532	1.0519	T_{68-69}	0.9174	0.9027	0.9049	0.9171
V_{g85} (p.u.)	1.0509	1.0506	1.0579	1.0622	T_{81-80}	1.0103	0.9486	0.9869	0.9813
V_{g87} (p.u.)	1.0466	1.0405	1.0493	1.0608					

	BBO	DE	KHA	OKHA
Loss (MW)	188.9462	194.9291	183.5578	179.3371
Voltage deviation (p.u.)	1.7533	1.4466	2.0423	2.4609
Computational time (s)	20.0940	17.5881	6.3946	6.1364

Table 9
Simulation result of different algorithms for loss minimization (IEEE 118-bus system with UPFC).

Control variables	BBO	DE	KHA	OKHA	Control variables	BBO	DE	KHA	OKHA
V_{g1} (p.u.)	1.0944	1.0732	1.0969	1.0998	V_{g89} (p.u.)	1.0979	1.0731	1.0861	1.0897
V_{g4} (p.u.)	1.0063	1.0356	1.0146	1.0332	V_{g90} (p.u.)	1.0810	1.0372	1.0534	1.0641
V_{g6} (p.u.)	1.0328	1.0587	1.0391	1.0562	V_{g91} (p.u.)	1.0799	1.0345	1.0507	1.0642
V_{g8} (p.u.)	1.0207	1.0484	1.0250	1.0467	V_{g92} (p.u.)	1.0772	1.0441	1.0688	1.0714
V_{g10} (p.u.)	1.0401	1.0508	1.0514	1.0499	V_{g99} (p.u.)	1.0505	1.0435	1.0495	1.0573
V_{g12} (p.u.)	1.0709	1.0667	1.0683	1.0662	V_{g100} (p.u.)	1.0584	1.0600	1.0596	1.0593
V_{g15} (p.u.)	1.0173	1.0451	1.0233	1.0418	V_{g103} (p.u.)	1.0377	1.0481	1.0405	1.0406
V_{g18} (p.u.)	1.0029	1.0306	1.0051	1.0257	V_{g104} (p.u.)	1.0237	1.0384	1.0221	1.0193
V_{g19} (p.u.)	1.0138	1.0357	1.0097	1.0339	V_{g105} (p.u.)	1.0169	1.0339	1.0144	1.0144
V_{g24} (p.u.)	1.0007	1.0276	1.0075	1.0254	V_{g107} (p.u.)	1.0015	1.0298	1.0034	1.0003
V_{g25} (p.u.)	1.0372	1.0195	1.0571	1.0568	V_{g110} (p.u.)	1.0009	1.0367	1.0132	1.0007
V_{g26} (p.u.)	1.0761	1.0662	1.0978	1.0997	V_{g111} (p.u.)	1.0086	1.0472	1.0219	1.0047
V_{g27} (p.u.)	1.0742	1.0784	1.0984	1.0999	V_{g112} (p.u.)	0.9785	1.0182	0.9920	0.9846
V_{g31} (p.u.)	0.9997	1.0429	1.0374	1.0574	V_{g113} (p.u.)	1.0255	1.0472	1.0231	1.0473
V_{g32} (p.u.)	0.9982	1.0357	1.0196	1.0430	V_{g116} (p.u.)	1.0203	1.0268	1.0568	1.0623
V_{g34} (p.u.)	0.9952	1.0359	1.0292	1.0540	QC_5 (p.u.)	−0.0002	−0.3257	−0.0044	−0.0023
V_{g36} (p.u.)	1.0254	1.0193	1.0357	1.0090	QC_{34} (p.u.)	0.0976	0.1372	0.1176	0.0457
V_{g40} (p.u.)	1.0229	1.0141	1.0346	1.0058	QC_{37} (p.u.)	−0.0062	−0.0019	−0.0007	−0.0004
V_{g42} (p.u.)	1.0076	1.0060	1.0222	0.9932	QC_{44} (p.u.)	0.0996	0.0960	0.0973	0.0988
V_{g46} (p.u.)	1.0166	1.0242	1.0360	1.0102	QC_{45} (p.u.)	0.0996	0.0955	0.0999	0.0991
V_{g49} (p.u.)	1.0711	1.0510	1.0579	1.0420	QC_{46} (p.u.)	0.0617	0.0246	0.0252	0.0677

Table 9 (*continued*)

Control variables	BBO	DE	KHA	OKHA	Control variables	BBO	DE	KHA	OKHA
V_{g54} (p.u.)	1.0525	1.0748	1.0913	1.0656	QC_{48} (p.u.)	0.0714	0.0002	0.0009	0.0166
V_{g55} (p.u.)	0.9989	0.9969	1.0067	1.0418	QC_{74} (p.u.)	0.0325	0.0558	0.0359	0.0944
V_{g56} (p.u.)	0.9959	0.9973	1.0063	1.0409	QC_{79} (p.u.)	0.1962	0.1940	0.1993	0.1969
V_{g59} (p.u.)	0.9971	0.9971	1.0069	1.0411	QC_{82} (p.u.)	0.1959	0.1934	0.1963	0.1985
V_{g61} (p.u.)	1.0372	1.0458	1.0409	1.0706	QC_{83} (p.u.)	0.0976	0.0995	0.0979	0.0999
V_{g62} (p.u.)	1.0505	1.0600	1.0511	1.0558	QC_{105} (p.u.)	0.1863	0.1952	0.0234	0.0529
V_{g65} (p.u.)	1.0453	1.0571	1.0475	1.0520	QC_{107} (p.u.)	0.0313	0.0344	0.0569	0.0095
V_{g66} (p.u.)	1.0227	1.0351	1.0667	1.0720	QC_{110} (p.u.)	0.0091	0.0123	0.0099	0.0550
V_{g69} (p.u.)	1.0760	1.0849	1.0916	1.0817	T_{8-5}	0.9914	0.9803	0.9982	0.9911
V_{g70} (p.u.)	1.0514	1.0219	1.0548	1.0578	T_{26-25}	1.0997	1.0923	1.0978	1.0991
V_{g72} (p.u.)	1.0384	1.0140	1.0516	1.0517	T_{30-17}	1.0071	0.9880	1.0128	0.9877
V_{g73} (p.u.)	1.0450	1.0171	1.0509	1.0506	T_{38-37}	0.9821	1.0094	0.9946	1.0210
V_{g74} (p.u.)	1.0401	1.0058	1.0416	1.0481	T_{63-59}	0.9657	0.9696	0.9824	0.9683
V_{g76} (p.u.)	1.0352	1.0089	1.0330	1.0421	T_{64-61}	0.9915	0.9927	1.0072	0.9932
V_{g77} (p.u.)	1.0597	1.0396	1.0606	1.0606	T_{65-66}	1.0903	1.0903	1.0983	0.9045
V_{g80} (p.u.)	1.0727	1.0523	1.0709	1.0730	T_{68-69}	0.9007	0.9120	0.9048	0.9016
V_{g85} (p.u.)	1.0586	1.0546	1.0647	1.0647	T_{81-80}	0.9428	0.9606	0.9617	0.9589
V_{g87} (p.u.)	1.0604	1.0531	1.0570	1.0588					

	BBO	DE	KHA	OKHA
Active power injected by UPFC (p.u.)				
Sending end	0.0364	0.0147	0.0446	0.0511
Receiving end	0.0289	0.0182	0.0392	0.0372
Reactive power injected by UPFC (p.u.)				
Sending end	0.0235	0.0109	0.0346	0.0164
Receiving end	−0.0205	0.0082	0.0361	−0.0186
Optimal location and parameters of UPFC				
Optimal position	100–106	103–110	108–109	103.105
Series source voltage (p.u.)	0.0643	0.0344	0.0613	0.0718
Series source phase angle (rad)	−0.2272	−0.4581	−0.1895	−0.3654
Shunt source voltage (p.u.)	1.0254	1.0537	1.0269	1.0450
Shunt source phase angle (rad)	−0.1954	−0.3216	−0.1058	−0.2552
Loss (MW)	181.3006	185.3712	178.4892	176.2346
Voltage deviation (p.u.)	1.7683	1.9044	2.2657	2.3178
Computational time (s)	22.6346	19.4245	8.5792	8.3699

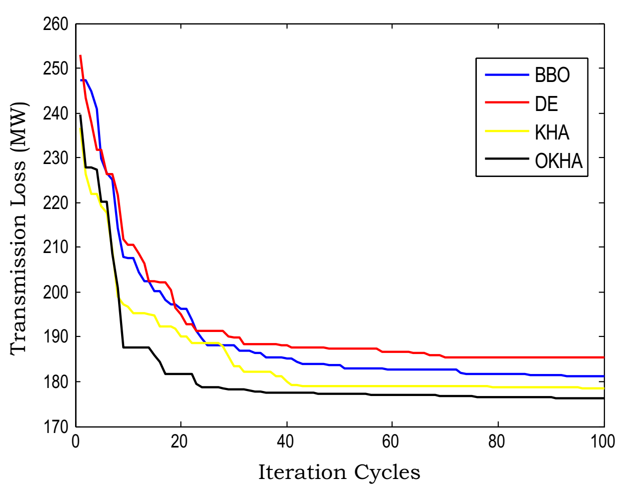

Fig. 4. Transmission loss convergence graph using different algorithms of IEEE 118-bus with UPFC.

Inequality constraints

In ORPD problem, the inequality constraints are the restrictions on transformer tap setting, reactive power generation, bus voltage and power flow through the transmission lines.

The independent variables of ORPD problem are the generator bus voltages, transformer tap position and the amount of reactive power source installation. These inequality constraints can be given as:

$$V_{G_f}^{\min} \leqslant V_{G_f} \leqslant V_{G_f}^{\max}, \quad f = 1, \ldots, N_G \tag{14}$$

$$Q_{C_f}^{\min} \leqslant Q_{C_f} \leqslant Q_{C_f}^{\max}, \quad f = 1, \ldots, N_C \tag{15}$$

$$T_f^{\min} \leqslant T_f \leqslant T_f^{\max}, \quad f = 1, \ldots, N_T \tag{16}$$

where $V_{G_f}^{\min}$, $V_{G_f}^{\max}$ are the minimum and maximum generator voltage of the fth bus respectively; $Q_{C_f}^{\min}$, $Q_{C_f}^{\max}$ are the minimum and maximum reactive power injection of the fth shunt compensator, respectively; $T_f^{\min}$, $T_f^{\max}$ are the minimum and maximum tap setting of the fth transmission line; N_G is the number of generators; N_C is the number of shunt compensators and N_T is the number of tap changing transformers.

The dependent variables of ORPD problem are the reactive power output of the generators, transmission line loading and load voltages. These constraints can be expressed as:

$$V_{L_f}^{\min} \leqslant V_{L_f} \leqslant V_{L_f}^{\max}, \quad f = 1, \ldots, N_L \tag{17}$$

$$Q_{G_f}^{\min} \leqslant Q_{G_f} \leqslant Q_{G_f}^{\max}, \quad f = 1, \ldots, N_G \tag{18}$$

$$S_{L_f} \leqslant S_{L_f}^{\max}, \quad f = 1, \ldots, N_{TL} \tag{19}$$

where $V_{L_f}^{\min}$, $V_{L_f}^{\max}$ are the minimum and maximum voltage of the fth load bus respectively; $Q_{G_f}^{\min}$, $Q_{G_f}^{\max}$ are the minimum and maximum reactive power generation of the fth generator bus respectively; $S_{L_f}^{\max}$ is the maximum apparent power flow in the fth line; N_L is the number of load buses.

Table 10
Simulation result of different algorithms for voltage deviation minimization (IEEE 118-bus system without UPFC).

Control variables	BBO	DE	KHA	OKHA	Control variables	BBO	DE	KHA	OKHA
V_{g1} (p.u.)	1.0798	1.0588	1.0428	1.0415	V_{g89} (p.u.)	0.9986	1.0179	1.0081	1.0092
V_{g4} (p.u.)	0.9829	1.0096	0.9876	1.0073	V_{g90} (p.u.)	0.9840	1.0953	1.0885	1.0129
V_{g6} (p.u.)	1.0267	0.9936	1.0268	0.9952	V_{g91} (p.u.)	0.9818	1.0874	1.0806	1.0048
V_{g8} (p.u.)	1.0181	1.0003	1.0263	1.0000	V_{g92} (p.u.)	1.0058	1.0676	1.0623	1.0152
V_{g10} (p.u.)	1.0430	1.0122	1.0416	0.9956	V_{g99} (p.u.)	1.0570	1.0004	1.0056	0.9901
V_{g12} (p.u.)	0.9515	0.9803	0.9509	0.9979	V_{g100} (p.u.)	1.0314	1.0269	1.0318	1.0217
V_{g15} (p.u.)	1.0188	1.0011	1.0239	1.0045	V_{g103} (p.u.)	1.0268	1.0988	1.0918	0.9799
V_{g18} (p.u.)	0.9979	0.9801	1.0005	0.9804	V_{g104} (p.u.)	0.9871	1.0755	1.0283	1.0497
V_{g19} (p.u.)	0.9633	0.9701	0.9768	1.0137	V_{g105} (p.u.)	1.0079	1.0444	0.9968	1.0186
V_{g24} (p.u.)	0.9829	0.9720	0.9952	0.9918	V_{g107} (p.u.)	0.9997	1.0688	1.0435	1.0250
V_{g25} (p.u.)	1.0187	1.0357	1.0122	1.0266	V_{g110} (p.u.)	0.9998	0.9830	1.0110	1.0291
V_{g26} (p.u.)	1.0967	1.0860	1.0995	1.0983	V_{g111} (p.u.)	1.0370	0.9531	0.9795	1.0788
V_{g27} (p.u.)	1.0983	1.0858	1.0481	0.9622	V_{g112} (p.u.)	1.0366	1.0391	1.0398	1.0807
V_{g31} (p.u.)	1.0092	1.0703	0.9928	1.0101	V_{g113} (p.u.)	1.0042	0.9976	1.0292	0.9924
V_{g32} (p.u.)	1.0026	1.0114	1.0108	1.0036	V_{g116} (p.u.)	1.0259	1.0898	1.0569	1.0160
V_{g34} (p.u.)	1.0014	1.0665	0.9835	1.0030	QC_5 (p.u.)	−0.3067	−0.0005	−0.3963	−0.3997
V_{g36} (p.u.)	1.0322	0.9824	1.0103	1.0056	QC_{34} (p.u.)	0.1127	0.0680	0.1267	0.1196
V_{g40} (p.u.)	1.0325	0.9896	1.0056	1.0014	QC_{37} (p.u.)	−0.1857	−0.0314	−0.2204	−0.2460
V_{g42} (p.u.)	1.0345	1.0107	0.9994	1.0076	QC_{44} (p.u.)	0.0502	0.0986	0.0981	0.0020
V_{g46} (p.u.)	1.0608	1.0009	1.0367	1.0155	QC_{45} (p.u.)	0.0182	0.0961	0.0564	0.0005
V_{g49} (p.u.)	1.0788	1.0391	1.0530	1.0746	QC_{46} (p.u.)	0.0812	0.0068	0.0292	0.0729
V_{g54} (p.u.)	1.0895	1.0446	1.0572	1.0631	QC_{48} (p.u.)	0.0068	0.0005	0.0024	0.0012
V_{g55} (p.u.)	1.0355	1.0232	1.0197	1.0492	QC_{74} (p.u.)	0.0177	0.0722	0.0748	0.0259
V_{g56} (p.u.)	1.0368	1.0215	1.0155	1.0439	QC_{79} (p.u.)	0.0483	0.0027	0.1776	0.0048
V_{g59} (p.u.)	1.0348	1.0242	1.0175	1.0482	QC_{82} (p.u.)	0.1574	0.1189	0.1986	0.1986
V_{g61} (p.u.)	1.0484	0.9754	1.0118	1.0350	QC_{83} (p.u.)	0.0788	0.0997	0.0974	0.0984
V_{g62} (p.u.)	1.0270	1.0041	1.0425	1.0394	QC_{105} (p.u.)	0.0686	0.0853	0.0429	0.1892
V_{g65} (p.u.)	1.0300	1.0150	1.0519	1.0462	QC_{107} (p.u.)	0.0582	0.0587	0.0153	0.0165
V_{g66} (p.u.)	1.0267	1.0925	1.0571	1.0145	QC_{110} (p.u.)	0.0103	0.0155	0.0427	0.0053
V_{g69} (p.u.)	0.9924	0.9589	0.9716	0.9760	T_{8-5}	1.0264	1.0030	1.0638	0.9828
V_{g70} (p.u.)	0.9972	1.0094	1.0330	1.0276	T_{26-25}	1.0273	1.0344	1.0918	1.0951
V_{g72} (p.u.)	1.0183	1.0191	0.9971	1.0088	T_{30-17}	0.9966	1.0140	0.9343	1.0315
V_{g73} (p.u.)	1.0066	1.0084	1.0106	1.0084	T_{38-37}	0.9367	0.9490	0.9037	0.9846
V_{g74} (p.u.)	0.9979	0.9977	1.0041	1.0069	T_{63-59}	0.9396	0.9929	0.9513	0.9538
V_{g76} (p.u.)	1.0067	1.0075	1.0084	1.0103	T_{64-61}	0.9741	0.9800	0.9788	0.9802
V_{g77} (p.u.)	1.0215	1.0256	1.0072	1.0087	T_{65-66}	0.9342	0.9058	1.0861	1.0979
V_{g80} (p.u.)	1.0268	1.0496	1.0237	1.0478	T_{68-69}	0.9125	0.9308	0.9000	0.9017
V_{g85} (p.u.)	1.0271	1.0037	1.0186	1.0166	T_{81-80}	0.9507	0.9610	0.9664	0.9162
V_{g87} (p.u.)	0.9855	1.0271	1.0044	1.0051					

	BBO	DE	KHA	OKHA
Loss (MW)	210.1989	230.1933	226.8364	219.1350
Voltage deviation (p.u.)	1.0250	1.1104	0.8588	0.7740
Computational time (s)	20.1347	17.4892	6.4700	6.1634

Algorithms

Krill herd algorithm

Krill herd algorithm (KHA) [25,26] is a novel meta-heuristic swarm intelligence optimization method for solving optimization problems, which is based on the simulation of the herding of the krill swarms in response to specific biological and environmental processes. The time-dependent position of an individual krill in 2D surface is governed by the following three main actions:

I. Movement induced by other krill individuals.
II. Foraging action.
III. Random diffusion.

These actions are briefly explain and mathematically expressed as follows:

Motion induced by other krill individuals

The direction of motion induced, α_i is approximately estimated by the target swarm density (target effect), a local swarm density (local effect), and a repulsive swarm density (repulsive effect). For a krill individual, this movement can be defined as follows:

$$M_i^k = \alpha_i M_i^{\max} + \omega_n M_i^{k-1} \tag{20}$$

where

$$\alpha_i = \alpha_i^{new} + \alpha_i^{target} \tag{21}$$

$$\alpha_i^{new} = \sum_{j=1}^{s} \Gamma_{i,j} \Psi_{i,j} \tag{22}$$

where

$$\Psi_{i,j} = \frac{x_i - x_j}{|x_i - x_j| + rand(0,1)} \tag{23}$$

$$\Gamma_{i,j} = \frac{F_i - F_j}{F_w - F_b} \tag{24}$$

$$\alpha_i^{terget} = 2\left(rand(0,1) + \frac{i}{i_{\max}}\right) \Gamma_i^{best} \Psi_i^{best} \tag{25}$$

where $M_i^{\max}$ is the maximum induced motion; M_i^k, M_i^{k-1} are the induced motion of the ith krill at the kth and $(k-1)$th movement; ω_n is the inertia weight of the motion induced; α_i^{new}, α_i^{target} are the local and the target effect, respectively; F_w, F_b are the worst and the best position respectively, among all krill individuals, of the

Table 11
Simulation result of different algorithms for voltage deviation minimization (IEEE 118-bus system with UPFC).

Control variables	BBO	DE	KHA	OKHA	Control variables	BBO	DE	KHA	OKHA
V_{g1} (p.u.)	1.0524	1.0433	1.0465	1.0192	V_{g89} (p.u.)	0.9993	1.0041	1.0120	1.0046
V_{g4} (p.u.)	1.0530	1.0180	0.9905	1.0036	V_{g90} (p.u.)	1.0677	0.9814	0.9513	1.0262
V_{g6} (p.u.)	1.0159	1.0496	1.0314	1.0115	V_{g91} (p.u.)	1.0679	0.9794	0.9569	1.0290
V_{g8} (p.u.)	1.0089	1.0587	1.0102	0.9996	V_{g92} (p.u.)	1.0506	1.0036	0.9832	1.0165
V_{g10} (p.u.)	1.0035	1.0804	1.0737	1.0052	V_{g99} (p.u.)	0.9717	1.0220	1.0070	0.9872
V_{g12} (p.u.)	0.9876	0.9520	0.9509	0.9852	V_{g100} (p.u.)	1.0021	1.0326	1.0390	1.0218
V_{g15} (p.u.)	1.0199	1.0412	1.0226	1.0086	V_{g103} (p.u.)	1.0534	0.9614	1.0938	1.0694
V_{g18} (p.u.)	1.0009	1.0158	1.0096	0.9910	V_{g104} (p.u.)	1.0260	1.0094	1.0421	1.0386
V_{g19} (p.u.)	1.0027	1.0421	1.0095	0.9944	V_{g105} (p.u.)	1.0040	1.0145	1.0099	1.0080
V_{g24} (p.u.)	1.0041	1.0223	1.0215	0.9998	V_{g107} (p.u.)	1.0500	1.0228	0.9975	1.0192
V_{g25} (p.u.)	1.0761	1.0384	1.0009	1.0412	V_{g110} (p.u.)	1.0033	0.9898	1.0129	0.9997
V_{g26} (p.u.)	1.0980	1.0494	1.0153	1.0379	V_{g111} (p.u.)	0.9784	1.0210	1.0636	0.9688
V_{g27} (p.u.)	1.0320	1.0072	1.0158	1.0111	V_{g112} (p.u.)	1.0603	1.0058	0.9732	1.0568
V_{g31} (p.u.)	1.0666	1.0153	1.0656	1.0603	V_{g113} (p.u.)	1.0061	1.0288	1.0471	1.0124
V_{g32} (p.u.)	1.0108	0.9973	1.0010	0.9972	V_{g116} (p.u.)	1.0092	1.0251	0.9857	0.9957
V_{g34} (p.u.)	1.0628	1.0106	1.0579	1.0516	QC_5 (p.u.)	−0.2875	−0.1697	−0.3347	−0.3694
V_{g36} (p.u.)	0.9727	1.0296	0.9964	1.0148	QC_{34} (p.u.)	0.0955	0.1266	0.1189	0.0893
V_{g40} (p.u.)	0.9825	1.0318	0.9951	1.0029	QC_{37} (p.u.)	−0.0100	−0.0699	−0.0707	−0.2496
V_{g42} (p.u.)	1.0157	1.0506	1.0125	1.0018	QC_{44} (p.u.)	0.0998	0.0423	0.0991	0.0067
V_{g46} (p.u.)	1.0275	1.0424	0.9990	1.0296	QC_{45} (p.u.)	0.0979	0.0505	0.0985	0.0102
V_{g49} (p.u.)	1.0389	1.0765	1.0330	1.0916	QC_{46} (p.u.)	0.0033	0.0153	0.0049	0.0292
V_{g54} (p.u.)	1.0483	1.0828	1.0506	1.0605	QC_{48} (p.u.)	0.0075	0.0055	0.0006	0.0013
V_{g55} (p.u.)	1.0394	1.0466	1.0356	0.9739	QC_{74} (p.u.)	0.0631	0.0071	0.0894	0.0274
V_{g56} (p.u.)	1.0347	1.0433	1.0291	0.9638	QC_{79} (p.u.)	0.0017	0.0309	0.0007	0.0088
V_{g59} (p.u.)	1.0372	1.0473	1.0339	0.9703	QC_{82} (p.u.)	0.1881	0.1746	0.1998	0.1980
V_{g61} (p.u.)	1.0726	1.0247	1.0432	1.0598	QC_{83} (p.u.)	0.0187	0.0990	0.0995	0.0947
V_{g62} (p.u.)	1.0142	0.9811	0.9990	0.9964	QC_{105} (p.u.)	0.1466	0.1617	0.1028	0.1195
V_{g65} (p.u.)	1.0189	0.9718	0.9985	0.9995	QC_{107} (p.u.)	0.0193	0.0263	0.0592	0.0114
V_{g66} (p.u.)	0.9901	1.0318	0.9964	0.9951	QC_{110} (p.u.)	0.0425	0.0193	0.0232	0.0312
V_{g69} (p.u.)	1.0013	1.0536	1.0176	1.0194	T_{8-5}	1.0235	1.0599	1.0445	1.0498
V_{g70} (p.u.)	1.0856	0.9961	0.9976	1.0033	T_{26-25}	0.9027	0.9224	1.0976	1.0903
V_{g72} (p.u.)	1.0690	1.0222	1.0074	1.0229	T_{30-17}	1.0131	1.0032	0.9003	0.9678
V_{g73} (p.u.)	1.0709	1.0088	1.0002	1.0080	T_{38-37}	0.9425	0.9013	1.0023	0.9961
V_{g74} (p.u.)	1.0802	1.0162	1.0049	1.0137	T_{63-59}	0.9409	1.0062	0.9629	0.9529
V_{g76} (p.u.)	1.0536	1.0093	1.0053	1.0027	T_{64-61}	0.9782	0.9517	1.0049	1.0009
V_{g77} (p.u.)	1.0189	1.0074	1.0122	1.0100	T_{65-66}	0.9001	0.9191	0.9023	0.9107
V_{g80} (p.u.)	1.0438	1.0374	1.0304	1.0293	T_{68-69}	0.9006	0.9017	1.0693	0.9750
V_{g85} (p.u.)	1.0237	1.0263	1.0130	1.0248	T_{81-80}	0.9165	0.9248	0.9423	0.9590
V_{g87} (p.u.)	0.9936	0.9909	1.0109	0.9908					

	BBO	DE	KHA	OKHA
Active power injected by UPFC (p.u.)				
Sending end	0.0261	0.0482	0.0277	0.0293
Receiving end	0.0235	0.0389	0.0178	0.0283
Reactive power injected by UPFC (p.u.)				
Sending end	0.0153	0.0275	−0.0164	0.0258
Receiving end	−0.0084	0.0146	0.0341	0.0106
Optimal location and parameters of UPFC				
Optimal position	62–67	49–69	49–69	65–68
Series source voltage (p.u.)	0.0614	0.0347	0.0285	0.0492
Series source phase angle (rad)	−0.1267	−0.0964	−0.3166	−0.2462
Shunt source voltage (p.u.)	1.0382	1.0543	1.0892	1.0630
Shunt source phase angle (rad)	−0.3194	−0.1358	−0.2203	−0.3677
Loss (MW)	210.6723	223.9840	218.1042	222.2589
Voltage deviation (p.u.)	1.0124	1.0312	0.7318	0.6742
Computational time (s)	22.5217	19.6005	8.4871	8.2870

population; F_i, F_j are the fitness value of ith and jth individuals, respectively; i is the current iteration number and i_{max} is the maximum iteration number.

To identify the neighboring members of each krill individual, a sensing distance (S_{d_i}) parameter is used. If the distance between the two individual krill is less than the sensing distance, that particular krill is considered as neighbor of the other krill. The sensing distance may be defined by:

$$sd_i = \frac{1}{5S}\sum_{j=1}^{S}|X_i - X_j| \tag{26}$$

where S is the number of krill individuals surrounding the particular krill; X_i, X_j are the position of the ith and jth krill, respectively.

Foraging action

The foraging motion $M_{f_i}^k$ is covered in terms of two main effective parameters. The first one is the current food location and the second one is the previous experience about the food location. This motion can be expressed for the ith krill individual as follows:

$$M_{f_i}^k = 0.02\beta_i + \omega_x M_{f_i}^{k-1} \tag{27}$$

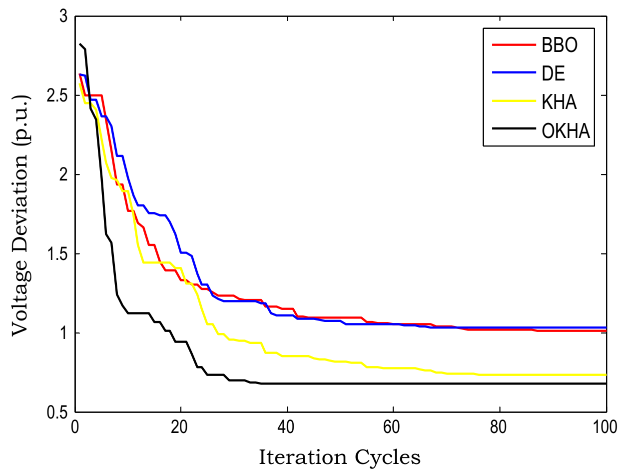

Fig. 5. Voltage deviation convergence graph using different algorithms of IEEE 118-bus with UPFC.

$$\beta_i = 2\left(1 - \frac{i}{i_{\max}}\right) F_i \frac{\sum_{j=1}^{s} \frac{x_j}{F_j}}{\sum_{j=1}^{N_S} \frac{1}{F_j}} + \Gamma_i^{best} \Psi_i^{best} \tag{28}$$

where ω_x is the inertia weight of the foraging motion; $M_{f_i}^{k-1}$, $M_{f_i}^{k}$ is the foraging motion of the ith krill at $(k-1)$th and kth movement.

Random diffusion

The diffusion process of the krill individuals is considered as a random phenomenon. It may be represented in terms of a maximum diffusion speed and a random directional factor and may mathematically be expressed by:

$$M_{d_i}^{k} = \lambda M_d^{\max} \tag{29}$$

where $M_d^{\max}$ is the maximum diffusion motion; λ is the directional vector uniformly distributed between $(-1, 1)$.

Position update

Finally, the position of the ith krill during the time interval t to Δt may be expressed as:

Table 12
Simulation result of different algorithms for simultaneous minimization of loss and voltage deviation (IEEE 118-bus system without UPFC).

Control variables	BBO	DE	KHA	OKHA	Control variables	BBO	DE	KHA	OKHA
V_{g1} (p.u.)	1.0154	0.9904	1.0137	0.987	V_{g89} (p.u.)	1.0789	1.0591	1.0375	1.074
V_{g4} (p.u.)	1.0259	1.0176	1.0798	1.0287	V_{g90} (p.u.)	1.0730	1.0440	0.9748	1.049
V_{g6} (p.u.)	1.0104	1.0208	1.0430	1.0415	V_{g91} (p.u.)	1.0212	1.0126	0.9898	1.0563
V_{g8} (p.u.)	1.0448	1.0309	1.0757	1.0518	V_{g92} (p.u.)	1.0225	1.0313	1.0155	1.0413
V_{g10} (p.u.)	1.0620	0.9714	1.0731	1.089	V_{g99} (p.u.)	1.0342	1.0658	1.0005	1.0707
V_{g12} (p.u.)	1.0109	1.0253	1.0377	1.0233	V_{g100} (p.u.)	1.0002	1.0647	1.0197	1.0485
V_{g15} (p.u.)	0.9798	1.0320	0.9971	1.0119	V_{g103} (p.u.)	1.0173	1.0598	1.0466	1.0413
V_{g18} (p.u.)	1.0127	1.0429	1.0281	0.9901	V_{g104} (p.u.)	1.0108	1.0484	1.0202	1.0031
V_{g19} (p.u.)	0.9794	1.0295	0.9975	1.0021	V_{g105} (p.u.)	1.0201	1.0556	0.9943	1.0083
V_{g24} (p.u.)	0.9956	1.0032	1.0573	1.0465	V_{g107} (p.u.)	0.9873	1.0924	1.0301	1.0117
V_{g25} (p.u.)	1.0419	1.0956	1.0944	1.0645	V_{g110} (p.u.)	0.9959	1.0069	1.0124	1.0352
V_{g26} (p.u.)	1.0631	1.0523	1.0964	1.0777	V_{g111} (p.u.)	1.0262	0.9966	1.0087	1.0362
V_{g27} (p.u.)	1.0059	1.0748	1.0097	1.0076	V_{g112} (p.u.)	1.0072	0.9894	0.9989	1.0364
V_{g31} (p.u.)	0.9835	0.9726	1.0432	0.9693	V_{g113} (p.u.)	1.0164	1.0629	1.0354	0.9898
V_{g32} (p.u.)	0.9927	1.0304	1.0245	1.0096	V_{g116} (p.u.)	1.0158	0.9954	1.0418	1.0073
V_{g34} (p.u.)	1.0277	1.0109	1.0206	1.0419	QC_5 (p.u.)	−0.1469	−0.3607	−0.0538	−0.3865
V_{g36} (p.u.)	1.0047	1.0065	0.9923	1.0551	QC_{34} (p.u.)	0.1256	0.1249	0.0208	0.094
V_{g40} (p.u.)	1.0096	1.0162	1.0259	0.9975	QC_{37} (p.u.)	−0.1059	−0.0643	−0.0740	−0.0352
V_{g42} (p.u.)	1.0142	1.0374	0.9890	0.9704	QC_{44} (p.u.)	0.0227	0.0203	0.0812	0.0104
V_{g46} (p.u.)	1.0675	1.0509	1.0235	1.0398	QC_{45} (p.u.)	0.0231	0.0535	0.0113	0.0952
V_{g49} (p.u.)	1.0562	1.0778	1.0253	1.0459	QC_{46} (p.u.)	0.0926	0.0149	0.0078	0.0523
V_{g54} (p.u.)	1.0370	0.9973	1.0196	1.0116	QC_{48} (p.u.)	0.0152	0.1118	0.0299	0.0649
V_{g55} (p.u.)	1.0200	1.0259	1.0145	0.9898	QC_{74} (p.u.)	0.1099	0.0920	0.1142	0.0993
V_{g56} (p.u.)	1.0228	1.0179	1.0202	0.9952	QC_{79} (p.u.)	0.1085	0.1722	0.0383	0.0809
V_{g59} (p.u.)	1.0514	1.0811	1.0130	1.0324	QC_{82} (p.u.)	0.1919	0.1852	0.1684	0.1333
V_{g61} (p.u.)	1.0554	1.0899	1.0605	1.0340	QC_{83} (p.u.)	0.0172	0.0583	0.0736	0.0013
V_{g62} (p.u.)	1.0607	1.0803	1.0254	1.0368	QC_{105} (p.u.)	0.0634	0.1921	0.0490	0.058
V_{g65} (p.u.)	0.9965	1.0464	1.0294	1.0129	QC_{107} (p.u.)	0.0071	0.0476	0.0491	0.0506
V_{g66} (p.u.)	1.0777	1.0896	1.0329	1.0596	QC_{110} (p.u.)	0.0094	0.0562	0.0202	0.0394
V_{g69} (p.u.)	1.0666	1.0684	1.0814	1.0811	T_{8-5}	1.0773	0.9679	1.0149	1.0151
V_{g70} (p.u.)	0.9745	1.0093	1.0141	1.0298	T_{26-25}	0.9788	0.9845	0.9858	1.0869
V_{g72} (p.u.)	1.0276	0.9696	1.0042	1.0463	T_{30-17}	1.0578	0.9194	0.9861	1.0113
V_{g73} (p.u.)	0.9703	1.0252	1.0516	1.0626	T_{38-37}	0.9506	1.0235	0.9511	0.9673
V_{g74} (p.u.)	0.9898	0.9698	1.0170	1.0296	T_{63-59}	1.0054	0.9001	1.0679	0.9527
V_{g76} (p.u.)	0.9868	0.9711	1.0281	1.0074	T_{64-61}	0.9933	0.9619	1.0130	0.9642
V_{g77} (p.u.)	1.0521	1.0078	1.0492	1.0314	T_{65-66}	0.9762	0.9552	1.0731	1.0268
V_{g80} (p.u.)	1.0469	1.0113	1.0421	1.0351	T_{68-69}	0.9054	0.9296	0.9353	1.0515
V_{g85} (p.u.)	1.0597	1.0205	1.0027	1.0260	T_{81-80}	1.0633	0.9849	0.9265	1.0085
V_{g87} (p.u.)	1.0121	0.9998	0.9959	1.0888					

	BBO	DE	KHA	OKHA
Loss (MW)	202.5037	205.1311	203.0830	194.9155
Voltage deviation (p.u.)	1.3035	1.3440	1.2888	1.2218
Computational time (s)	20.1372	17.9003	6.2712	6.1547

Table 13
Simulation result of different algorithms for simultaneous minimization of loss and voltage deviation (IEEE 118-bus system with UPFC).

Control variables	BBO	DE	KHA	OKHA	Control variables	BBO	DE	KHA	OKHA
V_{g1} (p.u.)	0.9944	1.0014	1.0022	0.9944	V_{g89} (p.u.)	1.0155	1.0163	1.0422	1.0955
V_{g4} (p.u.)	1.0223	1.0160	1.0311	1.0244	V_{g90} (p.u.)	1.0484	0.9507	1.0441	1.0662
V_{g6} (p.u.)	0.9918	0.9955	1.0006	1.0108	V_{g91} (p.u.)	1.0085	0.9939	1.0113	1.0603
V_{g8} (p.u.)	1.0169	0.9532	1.0067	1.0855	V_{g92} (p.u.)	0.9929	1.0379	1.0271	1.0708
V_{g10} (p.u.)	0.9791	1.0202	1.0775	1.0998	V_{g99} (p.u.)	0.9589	1.0623	1.0335	1.0572
V_{g12} (p.u.)	1.0037	1.0264	1.0004	1.0091	V_{g100} (p.u.)	1.0353	1.0393	1.0316	1.0717
V_{g15} (p.u.)	0.9747	1.0096	1.0302	1.0198	V_{g103} (p.u.)	1.0298	1.0493	1.0514	1.0715
V_{g18} (p.u.)	0.9952	1.0302	1.0388	1.0168	V_{g104} (p.u.)	1.0322	1.0909	1.0121	1.0712
V_{g19} (p.u.)	1.0102	1.0297	1.0145	1.0155	V_{g105} (p.u.)	1.0120	1.0108	0.9901	1.0639
V_{g24} (p.u.)	1.0602	1.0012	1.0260	1.0338	V_{g107} (p.u.)	1.0151	1.0688	1.0350	1.0470
V_{g25} (p.u.)	1.0154	1.0767	1.0834	1.0937	V_{g110} (p.u.)	0.9923	0.9845	1.0076	1.0617
V_{g26} (p.u.)	1.0106	1.0055	1.0437	1.0977	V_{g111} (p.u.)	1.0335	0.9548	1.0505	1.0643
V_{g27} (p.u.)	1.0293	0.9764	1.0104	1.0430	V_{g112} (p.u.)	0.9665	1.0482	0.9990	1.0565
V_{g31} (p.u.)	0.9936	1.0023	0.9865	1.0238	V_{g113} (p.u.)	1.0169	0.9997	1.0167	1.0459
V_{g32} (p.u.)	0.9865	1.0224	1.0155	1.0343	V_{g116} (p.u.)	1.0447	0.9628	1.0045	1.0573
V_{g34} (p.u.)	1.0288	1.0458	1.0118	1.0136	QC_5 (p.u.)	−0.1246	−0.2359	−0.2282	−0.0988
V_{g36} (p.u.)	0.9804	0.9961	1.0043	1.0081	QC_{34} (p.u.)	0.0056	0.0369	0.0211	0.0027
V_{g40} (p.u.)	1.0186	1.0126	1.0032	1.0065	QC_{37} (p.u.)	−0.1669	−0.0685	−0.1209	−0.0264
V_{g42} (p.u.)	0.9725	1.0076	1.0306	1.0185	QC_{44} (p.u.)	0.0747	0.0574	0.0691	0.0790
V_{g46} (p.u.)	1.0117	1.0161	1.0413	1.0355	QC_{45} (p.u.)	0.0300	0.0725	0.0901	0.0868
V_{g49} (p.u.)	1.0060	1.0040	1.0053	1.0457	QC_{46} (p.u.)	0.0285	0.0765	0.0613	0.0784
V_{g54} (p.u.)	1.0153	0.9972	1.0287	1.0090	QC_{48} (p.u.)	0.0313	0.0286	0.0070	0.0037
V_{g55} (p.u.)	1.0581	0.9901	1.0213	1.0149	QC_{74} (p.u.)	0.0050	0.0239	0.0749	0.0204
V_{g56} (p.u.)	1.0381	1.0130	1.0212	1.0128	QC_{79} (p.u.)	0.1214	0.1392	0.1379	0.1907
V_{g59} (p.u.)	1.0572	1.0130	1.0176	1.0300	QC_{82} (p.u.)	0.1633	0.1284	0.1812	0.1910
V_{g61} (p.u.)	0.9726	0.9998	0.9940	1.0078	QC_{83} (p.u.)	0.0874	0.0004	0.0693	0.0610
V_{g62} (p.u.)	0.9757	1.0187	0.9755	1.0193	QC_{105} (p.u.)	0.1791	0.1602	0.1595	0.1143
V_{g65} (p.u.)	0.9931	0.9612	1.0202	1.0637	QC_{107} (p.u.)	0.0036	0.0273	0.0036	0.0066
V_{g66} (p.u.)	1.0366	1.0078	1.0383	1.0629	QC_{110} (p.u.)	0.0201	0.0143	0.0400	0.0032
V_{g69} (p.u.)	1.0452	0.9836	1.0472	1.0621	T_{8-5}	0.9637	1.0182	0.9655	1.0435
V_{g70} (p.u.)	0.9853	1.0418	1.0302	1.0178	T_{26-25}	1.0374	1.0238	1.0667	1.0864
V_{g72} (p.u.)	0.9528	1.0120	1.0236	1.0165	T_{30-17}	0.9460	1.0712	0.9111	1.0224
V_{g73} (p.u.)	1.0137	0.9761	0.9579	1.0161	T_{38-37}	0.9608	1.0004	1.0491	1.0192
V_{g74} (p.u.)	0.9603	1.0065	0.9829	1.0052	T_{63-59}	0.9717	0.9654	0.9101	0.9696
V_{g76} (p.u.)	1.0323	1.0462	1.0264	0.9893	T_{64-61}	1.0211	1.0663	1.0328	1.0315
V_{g77} (p.u.)	1.0193	1.0171	1.0006	1.0068	T_{65-66}	0.9799	1.0715	0.9469	1.0253
V_{g80} (p.u.)	1.0416	1.0279	1.0355	1.0267	T_{68-69}	0.9436	0.9088	0.9549	0.9274
V_{g85} (p.u.)	1.0092	1.0399	1.0285	1.0451	T_{81-80}	0.9184	0.9454	0.9218	1.0076
V_{g87} (p.u.)	1.0005	1.0066	0.9964	1.0263					

	BBO	DE	KHA	OKHA
Active power injected by UPFC (p.u.)				
Sending end	0.0238	0.0417	0.0182	0.0295
Receiving end	0.0226	0.0429	0.0211	0.0284
Reactive power injected by UPFC (p.u.)				
Sending end	−0.0316	0.0206	0.0344	0.0267
Receiving end	0.0284	−0.0137	0.0224	0.0230
Optimal location and parameters of UPFC				
Optimal position	49–54	50–57	56–58	50–57
Series source voltage (p.u.)	0.0583	0.0982	0.0643	0.0695
Series source phase angle (rad)	−0.0828	−0.1042	−0.0837	−0.0571
Shunt source voltage (p.u.)	1.0346	1.0283	1.0498	1.0428
Shunt source phase angle (rad)	−0.1221	−0.1006	−0.0672	−0.0390
Loss (MW)	194.3421	197.0782	192.6608	190.3824
Voltage deviation (p.u.)	1.2842	1.3018	1.2715	1.1944
Computational time (s)	22.8240	19.7211	8.3772	8.3069

$$x_i(t+\Delta t) = x_i(t) + \Delta t\left(M_i^k + M_{f_i}^k + M_{d_i}^k\right) \tag{30}$$

where

$$\Delta t = c_p \sum_{i=1}^{N} (u_i - l_i) \tag{31}$$

where N is the total number of control variables; u_i, l_i are the upper and lower limits of the ith control variable; c_p is the position constant factor.

Moreover, to improve the behavior of the individual Krill, two adaptive genetic operators of DE are added to the proposed algorithm. These two operators are briefly described below:

Genetic operators

To improve the performance of the algorithm, genetic reproduction mechanisms are incorporated into the algorithm. The introduced adaptive genetic reproduction mechanisms are crossover and mutation which are inspired from the classical DE algorithm. These two operations are described as follow:

Crossover

In this process, depending on crossover probability, each krill individual interacts with others to update its position. The *j*th components of the *i*th krill may be updated by

$$\Psi_{i,j} = \begin{cases} \Psi_{r,j} & \text{if } rand < c_r \\ \Psi_{i,j} & \text{else} \end{cases} \quad \text{where } r = 1,2,3\ldots,i-1,i+1,\ldots,N_P \tag{32}$$

where $c_r = 0.2\Gamma_i^{best}$

Mutation

The mutation operation creates mutant vectors $\Psi_{i,j}^m$ by perturbing the vector $\Psi_{best,j}$ with the difference of two other randomly selected vectors $\Psi_{o,j}$ and $\Psi_{p,j}$ as per following equation.

$$\Psi_{i,j}^m = \Psi_{best,j} + \mu(\Psi_{o,j} - \Psi_{p,j}) \tag{33}$$

The updated position of $\Psi_{i,j}^{\text{mod}}$ is selected from $\Psi_{i,j}^m$ and $\Psi_{i,j}$ using mutation probability μ_p as follows:

$$\Psi_{i,j}^{\text{mod}} = \begin{cases} \Psi_{i,j}^m & \text{if } rand \leqslant \mu_p \\ \Psi_{i,j} & \text{if } rand > \mu_p \end{cases} \tag{34}$$

Opposition based learning

Various optimization techniques start with some initial solutions and gradually try to improve them by converging them towards optimal values. Whenever any predefined criteria are satisfied, the search process stops. In the absence of any priori information, random guesses are made for taking up an initial solution. The distance of the random initial guesses from the optimal solution determines the computational time of execution of the search algorithm. Opposition-based learning (OBL) introduced by Tizhoosh [27] is one of the most successful concepts in computational intelligence, which enhances the search abilities of the conventional population based optimization techniques in solving nonlinear optimization problem. The main idea behind OBL is to consider the opposite of an assumption or a guess and comparing it with the original assumption, thereby improving the chances to find a solution faster. By simultaneously checking the opposite solution, the chance of starting with a closer or fitter solution can be improved. The OBL concept is based on the opposite point and opposite number which are defined as the following:

Opposite number: Let $x \in [\alpha, \beta]$ be a real number. Its opposite number x^0 is defined by:

$$x^o = \alpha + \beta - x \tag{35}$$

Opposite point: Let $P(x_1, x_2, \ldots, x_T)$ be a point in T-dimensional space, where $x_r \in [\alpha_r, \beta_r]$, $\forall r \in \{1, 2, \ldots, T\}$. The opposite point $P^0(x_1^0, x_2^0, \ldots, x_T^0)$ is defined by its components:

$$x_r^o = \alpha_r + \beta_r - x_r \tag{36}$$

Opposition based optimization

Opposition based optimization is based on opposition-based initialization and opposition-based generation jumping which are briefly described below:

Opposition-based initialization. In absence of priori knowledge, the only choice to create an initial population is random number generation. Oppositional learning can be utilized to obtain a fitter starting candidate solution without any prior knowledge about the solutions.

Initialization of opposite population (*OP*) may be described as follows:

---

for $r = 1 : n_p$ (n_p = *population size*)
  for $s = 1 : n_d$ (n_d = *number of control variables*)
    $OP_{r,s} = a_s + b_s - P_{r,s}$
  end
end

Opposition-based generation jumping. A similar approach can be applied to the current population by which the evolutionary process can be forced to jump to a new solution candidate, which may be more fit than the current one. After generating a new population by using KHA, the opposite population is generated based on a jumping rate j_r.

Opposite population jumping based on jumping rate as described below:

---

if rand $(0,1) < j_r$ (j_r = jumping rate)
  for $r = 1 : n_p$ (n_p = population size)
    for $s = 1 : n_d$ (n_d = no of control variables)
      $OP_{r,s} = a_s + b_s - P_{r,s}$
    end
  end
end

Oppositional krill herd algorithm applied to ORPD problem

The procedure for implementing the OKHA algorithm in solving ORPD problem for minimization of active power loss and voltage deviations can be summarized as follows:

Step 1: Initialize all independent variables such as all generators' voltages, tap settings of regulating transformers, reactive power injections, the active and reactive power injected by UPFC devices, voltage of UPFC connected bus are randomly within their specified operating limits.

Step 2: Update the independent variables of each initial solution string using the following expression to generate oppositional population.

$$OP_{r,s} = a_s + b_s - P_{rs}$$

where $r = 1, 2, \ldots, n_p$; $s = 1, 2, \ldots, n_d$; $P_{r,s}$ is the *s*th independent variables of the *r*th vector of the population; $OP_{r,s}$ is the *s*th independent variables of the *r*th vector of the opposite population; n_p is the population size and n_d is the number of independent variables.

Step 3: Run the Newton–Raphson load flow analysis to determine the dependent variables such as 'slack bus power, load voltages, power flow through the transmission line, source voltages of series and shunt branches of the UPFC devices and check whether they satisfy the operating limits or not. If any of these parameters violate the operating limits; discard that population set and re-initialize the corresponding set. Depending upon the population size, several solutions are generated. Each feasible solution set represents the initial position of each krill individual.

Step 4: Evaluate the fitness values of the current population (P) and oppositional population (OP) sets.

Step 5: Select n_p number of fittest individuals from $\{P \cup OP\}$.

Step 6: Sort the solutions from best to worst.
Step 7: Select few best solutions for elitism.
Step 8: Evaluate the three motion index, namely, motion induced by other individual; foraging motion and random diffusion.
Step 9: Modify the non-elite krill individuals' position.
Step 10: Apply crossover and mutation to update the position of each non-elite krill individuals. The updated position of krill individual represents the different independent variables. The parameters which are optimized in the OKHA algorithm.
Step 11: Check whether the independent variables violate the operating limits or not. If any independent variable is less than the minimum level it is made equal to minimum value and if it is greater than the maximum level it is made equal to maximum level.
Step 12: Run Newton–Raphson load flow analysis to determine the dependent variables and check whether they satisfy the system operating constraints or not. Replace the infeasible solutions by the best feasible solutions.
Step 13: Evaluate the opposite population of the current population and calculate the fitness values of the opposite population based on a jumping rate j_r (i.e. jumping probability).
Step 14: Select n_p fittest individuals from the union of the current population and the opposite population.
Step 15: Go to Step 4 for the next iteration until termination criterion is reached.
Step 16: Finally, the optimal parameters such as generators' voltages, tap settings of regulating transformers, reactive power injections, the active and reactive power injected by UPFC devices, voltage of UPFC connected bus and the location of the UPFC incorporated bus that optimized by the OKHA algorithm are identified.

Simulation results and discussions

To check the feasibility of the proposed OKHA method it is tested on IEEE 57-bus and IEEE 118-bus test systems and to validate the performance of the proposed method, it is compared with DE, BBO and conventional KHA approaches. The program is written in MATLAB-7 software and executed on a 2.5 GHz core i3 processor with 4-GB RAM. For implementing the DE, BBO, KHA and OKHA population size of 50 and the maximum number of generation (iterations) of 100 are taken in the simulation study. Since the performance of any algorithm depends on its input parameters, they should be carefully chosen. After several runs, the following input parameters shown in Table 1 are found to be the best for the optimal performance of the DE, BBO, KHA and OKHA algorithms.

Test system 1

Test system 1 represent IEEE 57-bus system [28] which consists of 80 branches, 7 generator buses and 15 branches under load tap setting transformer. The possible reactive power compensation buses are 18, 25 and 53. The base load of the system is 1272 MW and 298 MVAR. The upper and lower voltage limits at all the buses are taken as 1.10 p.u. and 0.95 p.u., respectively. The tap setting limits of all the regulating transformer are set to 0.9 p.u. for lower bound and to 1.1 p.u. for upper bound. In order to analyze the system under stressed condition, active and reactive power demand of each load bus are multiplied by 1.25. The line flow limits of all the lines are taken as two times of the base case line-flows. The lower and upper limits of the series voltage sources of the UPFC are taken within the interval of 0–0.2 p.u., respectively, and the limiting values of the shunt voltage sources of the UPFC are taken in between 0 and 1.1 p.u. The phase angles of these sources are within the range of 0–2π. The shunt and series impedances of installed UPFC are taken as $(0.01 + j0.1)$ p.u. and $(0.001 + j0.2)$ p.u., respectively.

Single objective function

Case I: Loss minimization. The IEEE 57 bus system is first considered without the allocation of any UPFC device within it. The optimal values of the control variables including power loss and voltage deviation evaluated using the BBO, DE, KHA and OKHA technique are listed in Table 2. It can be seen that the proposed OKHA technique gives the best loss among all the techniques without violating any operating constraint limits. Furthermore, BBO, DE, KHA and OKHA approaches are applied to UPFC based ORPD problem to find the optimal rating and location of UPFC for minimizing the real power losses and the corresponding results are illustrated in Table 3. It is observed from the simulation results that the loss obtained by BBO, DE, KHA and OKHA method are 40.5535 MW, 41.3003 MW, 40.2431 MW and 39.8134 MW respectively for without UPFC. However, after incorporating the UPFC in optimal position, loss obtained by BBO (39.3640 MW), DE (40.7651 MW), KHA (39.3642 MW) and OKHA (38.4255 MW) methods are substantially reduced. It is also observed from Tables 2 and 3 that the proposed OKHA method gives much better transmission loss than BBO, DE and KHA algorithms for both the cases. The convergence graph of BBO, DE, KHA and OKHA for transmission loss objective in IEEE 57 bus system without UPFC is given in Fig. 2.

Case II: voltage deviation minimization. In order to further evaluate the performance of the proposed OKHA optimization technique, normal ORPD and UPFC based ORPD for voltage deviation minimization objective are investigated. The results obtained for this objective function by BBO, DE, KHA and OKHA are reported in Tables 4 and 5, respectively without and with UPFC. In this case, the sum of voltage deviations obtained by BBO, DE, KHA and OKHA methods are 1.0409 p.u., 1.1104 p.u., 1.0182 p.u. and 0.9954 p.u., respectively, without UPFC. As seen in Table 4, the sum of voltage deviations in this case has been greatly reduced in all load buses using OKHA compared to BBO, DE and KHA algorithms. The UPFC device is then optimally placed on IEEE 57 bus system using the discussed techniques to reduced the voltage deviation further. The voltage deviation minimizations obtained by BBO, DE, KHA and OKHA methods are 0.9743 p.u., 1.0249 p.u., 0.9278 p.u. and 0.8942 p.u., respectively. It clearly suggests that the OKHA technique produces better voltage deviation results as compared to other techniques. The voltage deviation convergence graph using different algorithms on the IEEE 57 bus with UPFC is shown in Fig. 3.

Multi-objective function

To assess the efficiency of the proposed algorithm, multi-objective problem which minimizes the transmission loss and voltage deviation simultaneously is carried out. The objectives of transmission loss and voltage deviation are typically non-commensurable and conflict with each other in this multi-objective optimization problem. It is generally impossible to identify a solution while simultaneously optimizing the objectives. Table 6 shows the optimal setting of control variables, loss and voltage deviation for IEEE 57-bus test system obtained using the various methods without incorporating any facts devices. It can be easily concluded from the simulation results that the proposed method has resulted with better best compromise solution for both transmission loss and voltage deviation. To reduce the transmission loss and voltage deviation further, a UPFC device is then optimally placed on the same test system using the discussed techniques. A comparison is made among the best compromise solution obtained from the proposed OKHA method and the solutions obtained by BBO, DE and KHA algorithms. The results of this comparison are shown in Table 7. As it is shown in Table 7, the results achieve from the presented OKHA method for the best transmission loss and voltage deviation are significantly reduced to those of the BBO, DE and KHA algorithms which demonstrates the reliability of the OKHA algorithm.

Test system 2

In order to further demonstrate the effectiveness and validate the feasibility of the proposed OKHA algorithm, simulations are carried out for ORPD problem in the IEEE 118-bus test system [29]. The network consists of 186 branches, 54 generator buses and 12 capacitor banks. Nine branches 8–5, 26–25, 30–17, 38–37, 63–59, 64–61, 65–66, 68–69, and 81–80 are tap changing transformers. The total real and reactive power demands for base case are 3668 MW and 1438 Mvar, respectively. However, to analyze performance of various techniques under stressed condition, active and reactive power demand of each load bus are increased by 25%. In this study, the limiting tap setting values for tap changers are between 0.9 and 1.1 p.u., the allowed voltage changes are between 0.95 and 1.1. The voltage limits of the series sources of the UPFC are taken as 0–0.2 p.u. and the lower and upper limits of the shunt voltage sources of the UPFC are 0 p.u. and 1.1 p.u., respectively. The phase angles of both series and shunt sources are within the range of $0–2\pi$. The shunt and series impedances of installed UPFC are taken as $(0.01 + j0.1)$ p.u. and $(0.001 + j0.2)$ p.u., respectively.

Single objective function

Case I: Loss minimization. The IEEE 118 bus system is first considered without the allocation of any UPFC device within it. The optimal values of the control variables including power loss and voltage deviation are evaluated using the OKHA technique and then compared against the values obtained using BBO, DE and KHA techniques. It can be seen from Table 8 that the active power losses achieved by the BBO, DE, KHA and OKHA algorithm without UPFC are equal to 188.9462 MW, 194.9291 MW, 183.5578 MW and 179.3371 MW, respectively which clearly suggests that the proposed OKHA technique gives the best loss among all the discussed techniques. Afterward, to judge the algorithms' performance under complicated environment, the UPFC device is incorporated in the same test system. The optimal results of the various methods are presented in Table 9. It can be observed in Table 9 that the optimal location of the UPFC device for improved secure results for loss minimization for BBO, DE, KHA and OKHA techniques are 100–106, 103–110, 108–109 and 103–105 respectively. It can also be observed that all the methods are able to reduce the transmission loss effectively by placing the UPFC in optimal positions. Moreover, the result in Table 9 shows that the proposed OKHA optimization method outperforms other optimization techniques in terms solution quality and computational time. The transmission loss convergence graph using different algorithms on the IEEE 118 bus with UPFC are shown in Fig. 4.

Case II: Voltage deviation minimization. The optimal solutions obtained by BBO, DE, KHA and OKHA for the objective of voltage profile improvement of IEEE 118 bus system of normal ORPD and UPFC based ORPD are given in Tables 10 and 11, respectively. It may be noted that all the control variables are in their specified limits. It is observed from the simulation results of Table 10 that even without incorporating UPFC the voltage deviations are substantially been reduced from 1.7533 p.u. to 1.0250 p.u. by BBO, 1.4466 p.u. to 1.1104 p.u. by DE, 2.0423 p.u. to 0.8588 p.u. by KHA and 2.4609 p.u. to 0.7740 p.u. by OKHA as compared to the previous case. However, it is also found that the reduction of voltage deviation is most significant for OKHA among all the algorithms. Moreover, from Table 11 is found after incorporating UPFC in optimal location the voltage deviation is improved from 1.0250 p.u to 1.0124 p.u. using BBO, 1.1104 p.u. to 1.0312 p.u. using DE, 0.8588 p.u. to 0.7318 p.u. using KHA, and 0.7740 p.u. to 0.6742 p.u. using OKHA. Therefore, it can be concluded that by installing proper size of UPFC at proper place, the voltage profile of the power system can significantly be improved. Moreover, it is observed that voltage profile improvement ability of OKHA is best among all the discussed algorithms. The voltage deviation convergence graph using different algorithms using UPFC is shown in Fig. 5.

Multi objective function

In order to validate the effectiveness of the proposed procedure for multi-objective problem, it is applied on IEEE 118-bus system to minimize the transmission loss and voltage deviation simultaneously. To validate the superiority, the proposed OKHA method is compared with the BBO, DE and KHA algorithms. The optimal control variable settings, transmission loss and voltage deviation obtained using various intelligent techniques are given in Table 12. It can be seen from Table 12 that the proposed OKHA technique gives the best compromising solutions among all the techniques without violating any operating constraint limits. Moreover, for minimizing the real power losses and voltage deviation further, a UPFC device is optimally placed on IEEE 118-bus system by the presented approaches. Results obtained by the proposed OKHA method are compared with KHA, BBO and DE methods which are summarized in Table 13. The simulation results clearly show that the best compromising transmission loss and voltage deviation obtained by the proposed OKHA approach is least compared with other methods which emphasizes its better solution quality.

Conclusion

ORPD is an important problem in power engineering which has discrete variables, nonlinear objective function, and nonlinear constraints. In this paper, ORPD is solved using BBO, DE, KHA and OKHA algorithms to minimize the voltage deviation and total transmission loss. Moreover, to reduce the voltage deviation and transmission loss further, UPFC devices are optimally placed using the same algorithms. The performance of the proposed algorithms are demonstrated through their evaluation on the IEEE 57-bus and IEEE 118-bus power systems. The simulation results show that OKHA has better searching ability to find optimal solution as compared to other algorithms. So, it is believed that the proposed OKHA approach is capable of efficiently and effectively solving reactive power dispatch problem and will become a promising candidate for the optimal UPFC allocation problem problems. Also it may be observed from simulation results that computational time of OKHA in all test cases is lesser than that of conventional KHA, BBO and DE. Considering all these results of the study it can be concluded that OKHA performs better, than other methods in terms of solution quality, convergence speed and computational time.

References

[1] Shahidehpour M, Alomoush M. Restructured electrical power systems: operation, trading and volatility. NY: Marcel Dekker Inc.; 2001.
[2] Alomoush M. Fixed transmission rights for inter-zonal and intra-zonal congestion management. IEE Proc Gener Transm Distrib 1999;146(5):465–77.
[3] North American Reliability Council (NERC). Available Transfer Definitions and Determinations. NERC Report, June 1996.
[4] FACTS Overview. Piscataway: IEEE Power Engineering Society/Cigre, IEEE Service Center; 1995 [Special Issue, 95TP108].

[5] Edris A. FACTS technology development: an update. IEEE Power Eng Rev 2000 (March):4–9.
[6] Gyugyi L, Schauder CD, Williams SL, Rietman TR, Torgerson DR, Edris A. The unified power flow controller: a new approach to power transmission control. IEEE Trans Power Deliv 1995;10(2):1085–97.
[7] Gyugyi L. Unified power flow concept for flexible AC transmission systems. IEE Proc-C 1992;139(4):323–32.
[8] Singh SN, Erlich I. Locating unified power flow controller for enhancing power system loadability. In: International conference on future power system; 2005. p. 1–5.
[9] Wang KP, Yurevich J, Li A. Evolutionary-programming-based load flow algorithm for systems containing unified power flow controllers. IEE Proc Gener Transm Distrib 2003;150:441–6.
[10] Arabkhaburi D, Kazemi A, Yari M, Aghaei J. Optimal placement of UPFC in power systems using genetic algorithm. In: IEEE international conference on industrial technology; 2006. p. 1694–9.
[11] Saravanan M, Slochanal SMR, Venkatesh P, Abraham PS. Application of PSO technique for optimal location of FACST devices considering system loadability and cost of installation. Power Eng Conf 2005:716–21.
[12] Lashkar Ara A, Kazemi A, Nabavi Niaki SA. Multiobjective optimal location of FACTS shunt-series controllers for power system operation planning. IEEE Trans Power Deliv 2012;27(2).
[13] Sawhney H, Jeyasurya B. Application of unified power flow controller for available transfer capability enhancement. Int J Electr Power Sys Res 2004;69:155–60.
[14] Alomoush Muwaffaq I. Impacts of UPFC on line flows and transmission usage. Int J Electr Power Sys Res 2004;71:223–34.
[15] Taher SA, Amooshahi MK. New approach for optimal UPFC placement using hybrid immune algorithm in electric power systems. Int J Electr Power Energy Syst 2012;43:899–909.
[16] Shaheen Husam I, Rashed Ghamgeen I, Cheng SJ. Optimal location and parameter setting of UPFC for enhancing power system security based on Differential Evolution algorithm. Int J Electr Power Energy Syst 2011;33:94–105.
[17] Vural AM, Tümay M. Mathematical modeling and analysis of a unified power flow controller: a comparison of two approaches in power flow studies and effects of UPFC location. Int J Electr Power Energy Syst 2007;29:617–29.
[18] Visakha K, Thukaram D, Jenkins L. Application of UPFC for system security improvement under normal and network contingencies. Int J Electr Power Syst Res 2004;70:46–55.
[19] Roy PK, Ghoshal SP, Thakur SS. Optimal reactive power dispatch considering FACTS devices using biogeography based optimization. Electr Power Compon Syst 2011;39(8):733–50.
[20] Panda S. Application of non-dominated sorting genetic algorithm-II technique for optimal FACTS-based controller design. J Franklin Inst 2010;347:1047–64.
[21] Edward JB, Rajasekar N, Sathiyasekar K, Senthilnathan N, Sarjila R. An enhanced bacterial foraging algorithm approach for optimal power flow problem including FACTS devices considering system loadability. ISA Trans 2013;52:622–8.
[22] Hassan LH, Moghavvemi M, Almurib HAF, Steinmayer O. Application of genetic algorithm in optimization of unified power flow controller parameters and its location in the power system network. Int J Electr Power Energy Syst 2013;46:89–97.
[23] Kumar GN, Kalavathi MS. Cat swarm optimization for optimal placement of multiple UPFC's in voltage stability enhancement under contingency. Int J Electr Power Energy Syst 2014;57:97–104.
[24] Radman G, Raje RS. Power flow model/calculation for power systems with multiple FACTS controllers. Int J Electr Power Syst Res 2007;77:1521–31.
[25] Gandomi AH, Alavi AH. Krill Herd: a new bio-inspired optimization algorithm. Commun Nonlin Sci Numer Simul 2012;17(12):4831–45.
[26] Mandal B, Roy PK, Mandal S. Economic load dispatch using krill herd algorithm. Int J Electr Power Energy Syst 2014;57:1–10.
[27] Tizhoosh HR. Opposition-based learning: a new scheme for machine intelligence. In: International conference on computational intelligence for modelling control and automation (CIMCA) Vienna. Austria, vol. 1; 2005. p. 695–701.
[28] The IEEE 57-bus test system. <http://www.ee.washington.edu/research/pstca/pf57/pg_tca57bus.htm>.
[29] The IEEE 118-bus test system. <http://www.ee.washington.edu/research/pstca/pf118/pg_tca118bus.htm>.